CONFIDENTIAL

Investigation of unsteady viscous-inviscid interaction schemes

Fırat M. Haciahmetoğlu

Master of Science Thesis

TU Delft Delft University of Technology

ECN

MSCCONFIDENTIAL

Investigation of unsteady viscous-inviscid interaction schemes

Master of Science Thesis

For the degree of Master of Science in Computer Simulations for Scientists and Engineers (COSSE) at Delft University of Technology

Author:

Fırat M. Haciahmetoğlu

Supervisors:

Dr. Hüseyin Özdemir

Dr. Duncan R. van der Heul

August 21, 2013

Faculty of Electrical Engineering, Mathematics and Computer Science · Delft University of Technology

The work in this thesis was supported by Energy Research Centre of the Netherlands. Their cooperation is hereby gratefully acknowledged.

Abstract

The common practice in the wind energy industry is to develop design tools that provide aerodynamical characteristics in breadth of seconds. At Energy Research Centre of the Netherlands (ECN), there has been also a research to develop its own design tool for both two dimensional and three dimensional unsteady incompressible flows. This approach is based on the idea of L. Prandtl, splitting the flow domain into two regions, where the viscosity plays an essential role and where the influence of the viscosity can be neglected. Both regions are formulated and discretized by certain theoretical and numerical considerations in such a way that overall run time stays in a reasonable limit for the users. However, the idea of splitting causes an essential need to couple both regions to obtain the whole flow field solution. The viscous-inviscid interaction schemes investigates *the best* possible coupling between two existing models/regions.

In literature, the research that has been done so far mainly focused on the steady flows. The interaction methods, algorithms, and interaction laws have been developed considering the steady flow. In this research, the whole viscous-inviscid interaction embodiment is reinterpreted in terms of the unsteady flow. This causes conceptual changes in the way the coupling occurs.

In this thesis, first of all, the coupling techniques have been re-derived for the unsteady flow. The main focus is kept on the quasi-simultaneous interaction method since it is shown to be a rapidly convergent technique when the steady flow is considered. However, this becomes questionable when the unsteady effects are taken into account. In this study, it has been observed that the embodiment used for the steady quasi-simultaneous method is no longer valid and both a new quasi-simultaneous algorithm and a new formulation are needed for unsteady flow. Unlike the steady case, in the unsteady flow, the approximation to the inviscid flow has a direct role on the final result since it does not vanish when a converged solution is obtained. Furthermore, the whole idea of a *converged solution* becomes questionable. This profound distinction leads to a new algorithm where the final result is computed by the inviscid flow model to compensate the physics that has to be sacrificed in order to approximate the inviscid flow.

The approximation to the inviscid flow is called the interaction law. The earlier approaches

have been using the thin-airfoil approximation when the quasi-simultaneous scheme is employed. However, considering the unsteady case, the role of interaction law becomes primarily important than it used to be. In the steady case, the interaction law has been served as an auxiliary tool which has no effect on the final solution only effecting the convergence rate. However, in the unsteady case, the interaction law has direct effect on the final solution. Therefore, a new interaction law is derived based on the panel method. A similar approach has been implemented in case of the fully simultaneous method in a quite recent publication by Drela [1] without any approximation to the inviscid flow. Also, Coenen [2] mentioned this approach briefly; however, she also implemented the thin-airfoil approximation. The fact that the interaction law is an approximation, inevitably points out that as long as the quasi-simultaneous method is employed, there will be a physical information loss. This implies that the new interaction law which is still an approximation but physically more accurate then the thin-airfoil model since it incorporates more physical information. The loss of the information is stemmed from ignoring the non-diagonal terms in the aerodynamic influence matrices.

Having defined the interaction law, the governing equations of the viscous model, the integral boundary layer equations, and the interaction law constitute a coupled system occurring in the quasi-simultaneous step of the unsteady quasi-simultaneous scheme. This coupled system is analysed and the effect of the interaction law on the behaviour of the system is investigated for the laminar flow. It has been observed that, without the interaction law, i.e. setting the interaction law coefficient to zero, two eigenvalues of the system become same and the third one becomes zero. This behaviour of the characteristic resembles the Van Dommelen Singularity discussed in Chapter 4.3. Van Dommelen and Shen stated that there is a finite-time singularity which reveals itself as a blown-up displacement thickness that causes an overall breakdown. However, since there is no rigorous criteria for this type of unsteady singularity, it is not possible to conclude something about this unsteady singularity based solely on the current results and the characteristics without any simulation. It can be concluded that, as expected, there is no Goldstein singularity observed when the wall shear stress, the skin friction, vanishes. Although there are two distinct eigenvalues, the system has three distinct eigenvectors which means the matrix is *not* defective. When the interaction law is implemented to the system, it has been observed that the matrix has three distinct, real eigenvalues and the system becomes *strictly hyperbolic*. Furthermore, the interaction law coefficient shows a dependence with time step size. An optimal step size can be found numerically which ensures that the system becomes strictly hyperbolic.

Table of Contents

Acknowledgements **v**

1 Introduction **1**
1-1 Problem Description 1
1-2 Research Methodology 3

2 Flow model in viscous region **5**
2-1 Boundary layer theory 5
2-1-1 Boundary layer on a flat plate 8
2-2 Two dimensional unsteady integral boundary layer equations 11

3 Flow model in inviscid region **15**
3-1 Mathematical Model 17
3-1-1 Boundary conditions 22
3-2 Effect of the boundary layer on potential flow 27
3-3 Weak formulation and discretization 29
3-3-1 Discretization of the wing/aerofoil problem 29

4 Viscous-inviscid interaction **31**
4-1 Interaction methods 33
4-2 Unsteady quasi-simultaneous method 41
4-3 Discussion about unsteady singularities 46

5 Quasi-simultaneous solution **49**
5-1 Hyperbolic partial differential equations 49
5-2 Coupled system 51

6 Results **59**

7 Conclusions and Discussions **65**

Bibliography **69**

Acknowledgements

Before starting to show my gratitude individually, first of all, I would like to thank Prof. Dr. Kees Vuik and Prof. Dr. Ulrich Rüde and all the people who have worked for the Erasmus Mundus programme "Computer Simulations for Science and Engineering" (COSSE) and made it possible for me to study in such great universities in Europe.

Beside a cosmopolitan view, a solid education, good memories and a liberated mind, being in Europe gave me a chance to know one really special person, my supervisor Hüseyin Özdemir. He is a kind of person that you find yourself wondering "Is it really possible that someone can be so generous and good?" However, eventually you find out that "Yes, it is possible." Whatever I say here will not suffice to indicate my gratitude for all the things that he has done for me since more than two years while I have been studying in Europe. Nevertheless, I would like to thank Dr. Hüseyin Özdemir for his assistance during the writing of this thesis and for everything that he has done for me.

I would like to thank my TU Delft supervisor Dr. Duncan van der Heul, for his endless patience and genuine interest that he showed with my thesis; especially with my technical writing, without him, there would be many mistakes that I possibly cannot recognize, even realize.

I also owe a debt of gratitude to my co-worker Henk Seubers; without the valuable contribution of him it would not have been possible to overcome many difficulties that I faced during my thesis. He was always kind, helpful and he never hesitated to share his knowledge with me.

Another person whom contributed my thesis in great depth is Arne van Garrel. I like to thank him for his generosity in sharing his experience to guide me. In addition, I like to thank Anıl Özdemir. Without him some important points would have gone without notice.

I also would like to take this opportunity to express my sincere gratitude to Energy Research Centre of the Netherlands for providing a perfect working environment with the generous care towards its interns.

Finally, I do not know how to put my gratefulness to my family in words, for they never stop supporting me. Thank you very much.

Energy Research Centre of the Netherlands, Petten — Fırat M. Haciahmetoğlu
August 21, 2013

"It is an illusion to suppose that something is known, when all we have is a mathematical formula of what has happened: it is only characterized, described; no more!"

— *Friedrich Nietzsche*

Chapter 1

Introduction

While the energy need is rapidly increasing, the limited amount of the fossil fuels endanger the future of whole industry and causes an essential need for new kinds of alternative energy resources. Wind, with its common usage, environmental-friendly nature and promising future, is seen as one of the most important of them. Wind power, which is the conversion of wind energy into a useful form of energy using wind turbines, has a great potential to meet the energy demands of the world in a sustainable way. Europe has been acting for decades as a pioneer in the wind energy area. According to recent statistics published by the European Wind Energy Association in 2012 (EWEA), the annual installations of wind power have increased steadily over the last 12 years, from 3.2 GW in 2000 to 11.9 GW in 2012 with a compound annual growth rate of over 11.6 % in Europe and the total installed power capacity increased by 29.2 GW to 931.9 GW and reached a share of total installed generation capacity of 11.4 % of Europe. Besides the contribution to energy demand, 106 million tones of carbon dioxide per year were avoided, equivalent to taking 25% of cars in the EU off the road, using wind energy instead of fossil fuel.

Hence, it is evident that the wind turbines are becoming more and more a viable choice in terms of both energy and environmental issues. One of the main tasks of the Energy Research Centre of the Netherlands (ECN) Wind Energy Unit is to help the wind energy industry to improve existing designs to benefit most. The main attention is focused on the development of an advanced numerical scheme that can accurately predict the aerodynamic characteristics of a wind turbine rotor for incompressible two and three dimensional, steady and unsteady flows [3–5].

1-1 Problem Description

Predicting the characteristics of an unsteady flow around an arbitrary body by solving the Navier-Stokes equations coupled to a turbulence model is the common practice in the aerospace industry. However this process requires intensive computational effort when it comes to simulate large geometries. In the wind energy industry, on the other hand, the

aerodynamic characteristics of a wind turbine rotor is the main concern, in order to calculate the loadings on the blade, and these rotors have diameter ranging from 40 meter to 200 meter which causes huge computational domains. Using the common approach, the simulation of a single rotor will take days or months. However, it is not possible to wait for such a long time to provide a single result in the wind energy industry. Therefore, the algorithms developed to predict the aerodynamic characteristics of a wind turbine rotor, which are also called *design codes* in wind energy industry, are designed to provide reasonable results in breadth of seconds or minutes using a different approach then solving the full Navier-Stokes equations. The common approach to practise this in the wind industry is, following Prandtl's idea [6], to split the solution domain into an inner region that represents the viscous boundary layer and an outer region that models the inviscid external flow and solving them separately.

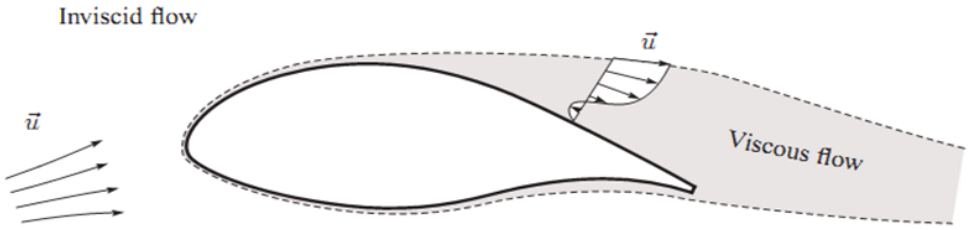

Figure 1-1: *Splitting of the flow domain into the viscous and inviscid regions.*

However, the splitting of the flow domain is an fictitious idea to facilitate the mathematical difficulties faced during the last century, namely the Navier-Stokes equations. In the nature, for a flow around an arbitrary body, it is not possible to observe a potential flow disjoint from its boundary layer. These two interact with each other, exchange information via pressure, density, temperature *etc.* and determine their characteristics as a whole. There is a reciprocal action between them. This brings about an essential need to couple these two regions which constitutes the main research subject of this thesis: *viscous-inviscid interaction (VII)* schemes.

At the Wind Energy unit of the Energy Centre of the Netherlands, ROTORFLOW project [3–5] has been initiated and still going on to develop ECN's own design tool for both two and three dimensional unsteady incompressible flows based on this splitting approach which has been used for almost one hundred year. For steady case, ECN has already developed design codes for the prediction of the aerodynamic characteristics on the wind turbine rotor. However, ignoring the unsteady motion of an airfoil effects directly the prediction of onset of the dynamic stall, which, consequently, yields poor overall design predictions. Hence, in the wind energy industry, unsteady effects have become of a great importance recently.

A great amount of research has been conducted on the splitting approach and therefore many results are available in literature for steady case (e.g. Balleur [7], Wigton and Holt [8], Houwink and Veldman [9], Drela and Giles [10], Cebeci *et al* [11], Nishida [12], Coenen [2], Bijleveld [13]). On the other hand, the unsteady flow is a relatively new research topic and a limited number of publications is available (e.g. Swafford *et al* [14], Cebeci *et al* [15], Bermudes *et al* [16], Garcia [17], Drela [1]).

The main target of this master thesis is to develop a *fast and accurate* viscous-inviscid inter-

action (VII) scheme between the viscous and inviscid solvers for unsteady, two dimensional, incompressible flow.

The performance of the coupling scheme directly depends on the treatment of the viscous and the inviscid regions. In order to maintain the overall efficiency, the modelling of these both regions are needed to be done in such a way that they also provide fast and accurate results within the regions they are employed. For this reason, the integral boundary layer formulation is used with the discontinuous Galerkin method discretization to model viscous part and the potential flow theory is employed with the panel method discretization to model the inviscid flow [3–5]. The VII schemes can be thought as a function of both the formulation and discretization of these two regions.

In this thesis, the flow is restricted to be 2D, unsteady, and incompressible and the optimal VII scheme is aimed to be developed. In literature, for steady case, the viscous-inviscid interaction has been investigated widely (e.g. Lock and Williams [18], Williams [19]) and also for unsteady case a limited amount of literature is available (e.g van Dommelen and Shen [20], Henkes and Veldman [21]) and the main methods have been listed as below:

- The direct method (e.g. Stewartson [22], Goldstein [23])
- The simultaneous method (e.g. Nishida [12], Drela [1])
- The quasi-simultaneous method (e.g. Veldman [24], Coenen [2])
- The inverse method (e.g. Catherall and Mangler [25])

Every method has its own advantages and disadvantages and all are explained in this thesis. However, a special attention is paid on Veldman's [24] the quasi-simultaneous scheme since it appears to be the most merit candidate for a fast and accurate overall solution. This method contains an approximation to the inviscid flow model to solve simultaneously with the viscous flow model. It has been successfully shown to be the fastest and the most accurate interaction scheme for steady case *under some assumptions* in [26] and [27]. However, for unsteady case, the usability of the quasi-simultaneous method has not yet been investigated which is investigated in this thesis.

1-2 Research Methodology

It has been stated that the efficiency of the viscous-inviscid schemes are determined by the mathematical properties of the models used in both viscous and inviscid regions. Therefore, the research begins with reviewing the physics and deriving the governing equations of these two regions. Chapter 2 explains the boundary layer concept and briefly introduces the integral boundary layer formulations. Then the final set of the unsteady integral boundary layer equations derived by Seubers [28] are given. This chapter is kept brief and for the details, the reader should refer to [28], since the current research is not focused on the derivation of the viscous flow region which is a broad subject. Chapter 3 presents detailed information about the modelling of the flow in the inviscid region. The potential flow model and the panel method are investigated and the general solution procedure is explained. In this chapter,

a detailed derivation is given since the coupling scheme, the quasi-simultaneous method, introduces an approximation to inviscid flow, namely the interaction term. A solid background of the modelling of the inviscid flow is needed to be able to derive an approximation to it. Chapter 4 describes the different VII methods that have been reported in the literature. For unsteady case, the quasi-simultaneous method is investigated in detail and a new algorithm and formulation are derived. Furthermore, the singularities within the unsteady boundary layer is discussed. In Chapter 5, the quasi-simultaneous solution which is a part of the unsteady quasi-simultaneous scheme is focused. The coupled system resulted from this quasi-simultaneous solution is analysed. Chapter 6 gives the results of the analysis of the coupled system and the effect of the interaction law on this system in the unsteady flow. Chapter 7 concludes the research, discusses the simplifications that have been done during the derivation of a new unsteady VII method and explains briefly the procedure to further the research.

Chapter 2

Flow model in viscous region

The Third International Congress of Mathematicians, organised in Heidelberg in 1904, hosted a physicist who had a revolutionary impact on the study of fluid mechanics. His name was Ludwig Prandtl. During the congress, he delivered a lecture and represented his paper entitled "*Über Flüssigkeitsbewegung bei sehr kleiner Reibung*[1]". In this paper, he successfully showed that it was possible to analyse viscous flows by making several theoretical considerations and simple experiments. Until that date, the science of theoretical hydrodynamics, which had evolved from Euler's equations of motion for a frictionless non-viscous fluid, and experimental results were in a great contradiction. Theory neglected the fluid friction due to overwhelming mathematical difficulties connected with the solution of the well-known Navier-Stokes equations. However, since the viscosities of most commonly used fluids, e.g. water and air, are very small, it was assumed that neglecting frictional forces, compared to remaining gravity and pressure forces, may not cause a profound effect on the general motion of fluid.

Prandtl was the first scientist who unified theoretical and experimental results by showing a new concept which took the fluid friction into consideration. He showed that the flow around a slender body can be divided into two regions: a very thin layer near to the body, *the boundary layer*, and remaining region outside this layer where the flow is named *the potential flow*. While in the former one, friction plays an essential role, in the latter one the fluid behaves as if it were inviscid. Prandtl supported his theorem with simple experiments performed in a small water tunnel. This was the first successful reunification of theory and experiment, which lead to great developments in the future [6].

2-1 Boundary layer theory

The characteristics of the flow around a solid object highly depend on various physical parameters such as size, orientation, speed, and fluid properties. The main non-dimensional expressions which characterize the influence on flows, however, depend on all these parameters and can be obtained by means of similarity, which dictates that for two flows around

[1] "On the motion of fluids of very small viscosity"

geometrically similar objects but having different parameters, forces acting on a fluid particle must have a fixed ratio to be similar. If we are to limit our interest only to frictional and inertia forces, to be similar, at all corresponding points the ratio of inertia and friction forces must be the same:

$$\frac{\text{Inertial Forces}}{\text{Frictional Forces}} = \text{constant}. \tag{2-1}$$

Osborne Reynolds was the one who first discovered that principle which essentially leads to a dimensionless number, known as the *Reynolds number*. The mathematical form of the Reynolds number is given by:

$$Re = \frac{\rho U d}{\mu}, \tag{2-2}$$

where ρ is the density, μ is the dynamic viscosity, U is the free stream velocity, d is the characteristic linear dimension of the body.

Recall that the Reynolds number represents the ratio of inertial effects to viscous effects, when the viscous effects are not taken into consideration, the Reynolds number approaches infinity. Similarly, in the absence of inertial effects, the Reynolds number is zero. It can be clearly concluded that any real flow will have a Reynolds number between these two extremes. The magnitude of the Reynolds number has a great effect on the nature of the flow.

When the Reynolds number is considerably less than one, this means that friction forces are dominant. In this type of flows, viscous effects are important in a large area around the object. The effect of Reynolds number can be clearly seen from Figure 2-1 where the flow past three flat plates of the same length l with Reynolds numbers of $0.1, 10, 10^7$ is shown.

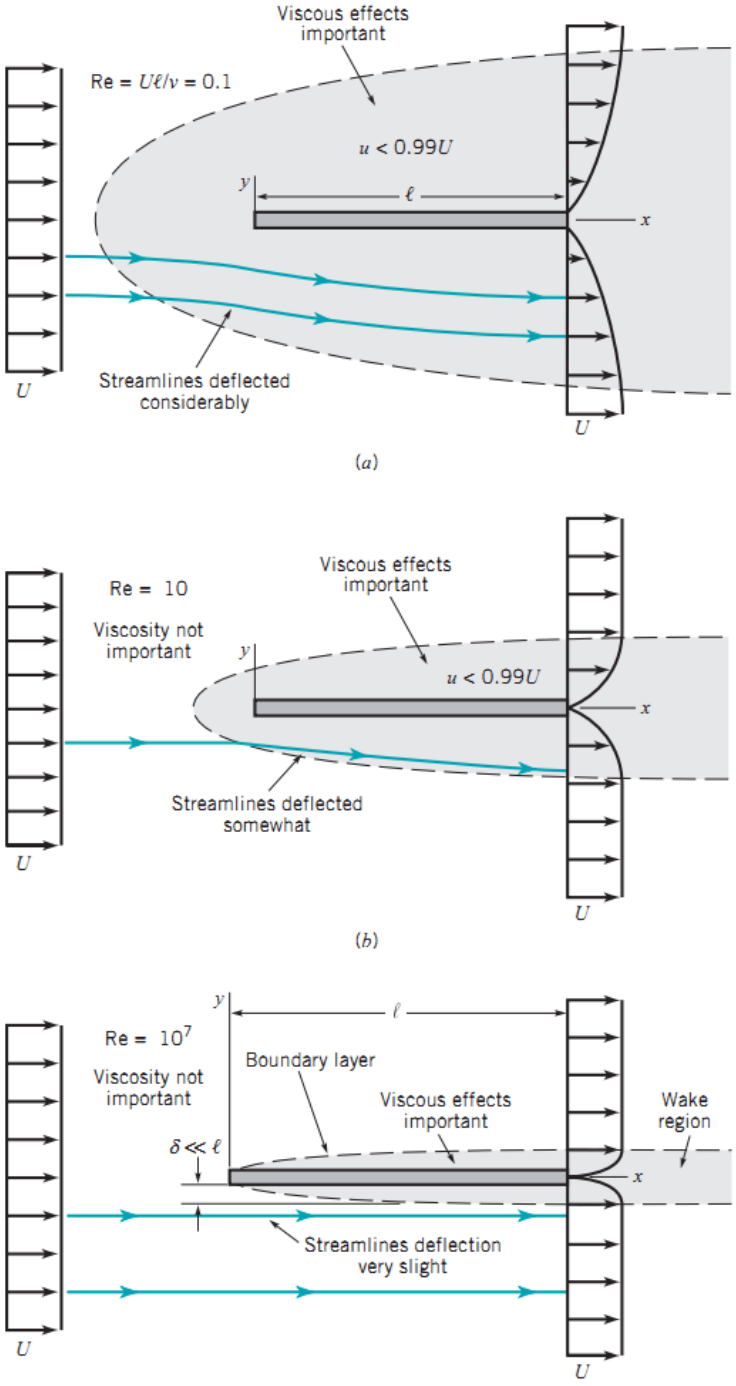

Figure 2-1: *Flows over a flat plate with various Reynolds numbers and the effect on viscous region within the flow field, reproduced from [29].*

The influence of viscosity at large Reynolds numbers is negligible everywhere except in a very thin layer in the immediate neighbourhood of the flat plate (solid wall) where the velocity increases from zero at the wall to its free stream value which corresponds to the external

frictionless flow to satisfy the no-slip boundary condition. The height of this thin layer is called the *thickness of the boundary layer*, δ, which increases from zero at the leading edge along the plate in the downstream direction. Figure 2-2 shows the velocity distribution in such a boundary layer.

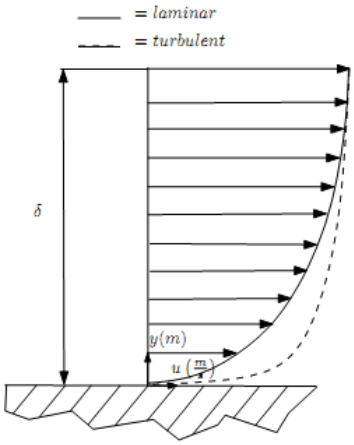

Figure 2-2: *Velocity distribution within a typical laminar and turbulent boundary layer profile along a flat plate.*

What Prandtl suggested was dividing the domain of the flow in the case of fluids of small viscosity into two regions: *the thin boundary layer* near the wall and the outside region where the fluid behaves essentially as if it were *inviscid*. This approximation brought great mathematical simplifications and became one of the corner-stones of modern fluid dynamics.

2-1-1 Boundary layer on a flat plate

The simplest example of boundary layer theory is presented by the flow along a very thin flat plate. Also, this example was the one that Prantdl used to illustrate his boundary layer theory.

The flow in the boundary layer can exist in three different regimes: laminar, transitional, and turbulent depending on the local Reynolds number. The velocity gradient in the boundary layer distorts the fluid particles. Since there is no velocity difference outside the viscous layer, the flow is irrotational. However, in the boundary layer, the flow becomes rotational which causes fluid particles, at some distance downstream from the leading edge, to be distorted greatly due to the random and irregular nature of the turbulence. Fluid particles, distorted or not, may separate from the boundary layer depending on the pressure distribution in the boundary layer. Fluid particles are accelerated beyond the stagnation point when the flow encounters a blunt body e.g. around a circular cylinder or flat plate with a thickness, and when the velocity increases, by momentum conservation, the pressure decreases. However, while this phenomenon occurs in the boundary layer, at the same time viscous forces dissipate the energy of the particles. In the end, the particles will lack sufficient momentum to surmount the required pressure level to continue on their streamline. They detach from the surface which is called "*boundary layer separation*".

In the boundary layer theory, there are three main parameters defined in such a way that they correspond to the physical quantities.

Boundary layer thickness, δ_ψ, is the orthogonal distance from the solid surface where the velocity in the boundary layer reaches some arbitrary fraction of the freestream velocity of the upstream velocity or the stream surface (in case of the interacting boundary layer). Typically, it is given as follows:

$$\delta_\psi = y \qquad where \qquad u = 0.99U. \tag{2-3}$$

where U is the velocity of incoming flow and for high Reynolds numbers, it becomes very thin, $\delta_\psi \ll L$. However, this has no practical importance since it is an arbitrary formulation (i.e. why %99, not %98?). Introducing the boundary layer edge $U_e = u|_{y=\delta_\psi}$, a formal definition can be suggested.

Boundary layer displacement thickness, δ^*, is defined to be used in calculations instead of boundary layer thickness since it is less arbitrary:

$$\delta^* = \int_0^{\delta_\psi} \left(1 - \frac{u}{U_e}\right) dy. \tag{2-4}$$

This expression represents the outward displacement of the streamlines caused by the viscous effects on the plate. In other words, the outward displacement of the wall that would be needed to obtain the same solution for the flow outside the boundary layer. This definition holds true for any incompressible flow, whether laminar or turbulent, constant or variable pressure. The physical interpretation of this thickness is illustrated below in Figure 2-3.

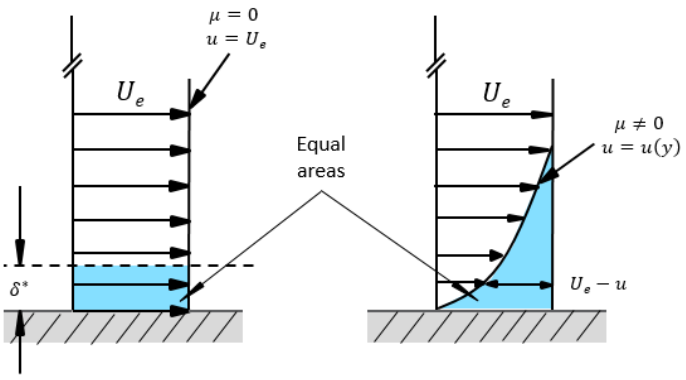

Figure 2-3: *Displacement thickness.*

Boundary layer momentum thickness, θ, is similar to the displacement thickness. It denotes the transverse distance over which the solid wall has to be displaced such that an inviscid flow produces the same momentum transport:

$$\theta = \int_0^{\delta_\psi} \frac{u}{U_e}\left(1 - \frac{u}{U_e}\right) dy. \tag{2-5}$$

This definition is applicable to any arbitrary incompressible boundary layer. It is important to note that θ is not a fundamental quantity as δ^* and only used in certain empirical correlations.

A physical representation of these three displacements thicknesses is given in Figure 2-4.

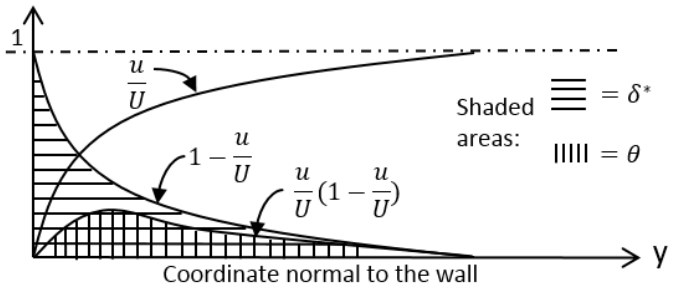

Figure 2-4: *Momentum and displacement thicknesses [30].*

The ratio between δ^* and θ is called the *shape factor* and given as

$$H = \frac{\delta^*}{\theta}. \tag{2-6}$$

The value of the shape factor varies with the profile of the flow and reliably indicates when the flow stays attached or will separate.

Another important parameter in boundary layer characterization is the friction coefficient, which represents the effect of wall shear forces on the flow, defined as

$$C_f(x) = \frac{\tau_w(x)}{\frac{1}{2}\rho U^2}, \tag{2-7}$$

where $\tau_w(x)$ is the wall shear stress on the plate, expressed as

$$\tau_w(x) = \mu \frac{\partial u}{\partial y}|_{y=0}, \tag{2-8}$$

where μ is the dynamical viscosity.

The background of the boundary layer theory has been briefly introduced above. However, the flow within the boundary layer can be solved following different approaches causing to define additional expression, parameters *etc.* The integral boundary layer approach is one of the most commonly used ones in the wind energy industry due to the short time expectations of the design procedure. This approach reduces the dimension of the problem by one at the

expense of additional closure relations obtained experimentally. A wide collection of integral boundary layer methods with different closure relations can be found in Es [31].

The model based on this thesis is derived following the unsteady integral boundary layer approach by Seubers [28].

2-2 Two dimensional unsteady integral boundary layer equations

Prandtl derived the boundary layer equations considering the asymptotic behaviour of the Navier-Stokes equations because at that time there were no other ways to find an approximate solution to this non-linear system of partial differential equations. The derivation of the integral boundary layer (IBL) equations may be initiated from this asymptotic form or it may also be started with the integral form of the Navier-Stokes equations. Seubers [28] followed the latter approach and derived a final set of governing equations in terms of conserved and asymptotic variables. Note that, the reader is advised to see [28] for detailed derivation. Within this chapter, the derivation is kept as simple as possible and concentrated on the final form of the governing equations since the derivation of the IBL equations are quite tedious and not of primary importance in this thesis.

Seubers used an Euler frame of reference and followed a control volume approach which is restricted in y direction by the streamline that passes along the boundary layer thickness and the wall and in x direction by two perpendicular lines to the wall at x_a and x_b. Then he formulated a mass and momentum balance for the control volume illustrated in Figure 2-5

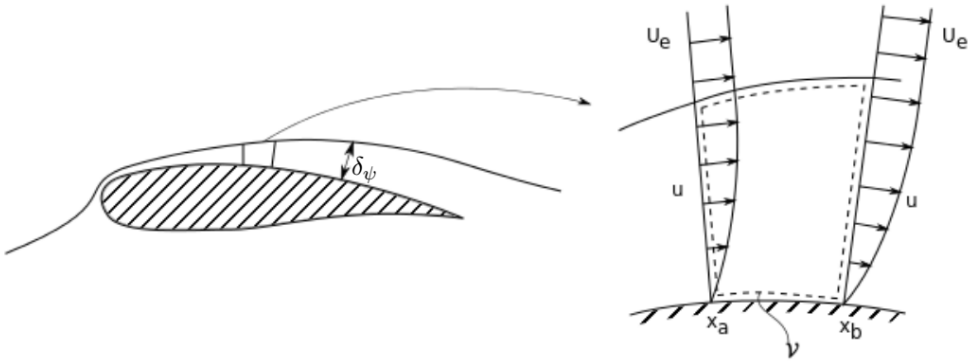

Figure 2-5: *The control volume for two dimensional flow [28].*

Despite the fact that in incompressible flow, the combination of an equation for the mass and momentum conservation suffices to formulate a closed model, the energy equation has also been considered in this approach. It is employed in order to control the dissipation to ensure that even one dimension is reduced (due to the integral boundary layer formulation), the system still conserves the mass, momentum and the energy.

The need for the closure relations arises from the fact that there are more unknowns than the number of equations in the system resulted from the fact that the Navier-Stokes equations are integrated in a direction orthogonal to the flow direction. By relating the additional

unknowns to one of the variables given in the system, an extra equation can be derived and used to solve the system. There are several closure relations proposed by different researchers. For the laminar flow, Thwaites method [32], one of the most commonly used laminar closure, is used. Other relations are derived by relating momentum density to both mass flux and momentum flux.

After a tedious derivation and employing the closure relations, the resulting set of equations in terms of asymptotic variables given below. The definitions of the each symbols is also given. Note that the **bold** notation corresponds to vector quantity.

The system in integral formulation:

$$\frac{\partial}{\partial t}\int_{\mathcal{V}} \boldsymbol{f}^t(\boldsymbol{u})\mathrm{d}\mathcal{V} + \int_{\mathcal{V}} \boldsymbol{g}^t(\boldsymbol{u})\frac{\partial \boldsymbol{u}}{\partial t}\mathrm{d}\mathcal{V} + [\boldsymbol{f}^x(\boldsymbol{u})]_{\partial\mathcal{V}^-}^{\partial\mathcal{V}^+} + \int_{\mathcal{V}} \boldsymbol{g}^x(\boldsymbol{u})\frac{\partial \boldsymbol{u}}{\partial x}\mathrm{d}\mathcal{V} = \int_{\mathcal{V}} \boldsymbol{s}(\boldsymbol{u})\mathrm{d}\mathcal{V}. \tag{2-9}$$

And the definitions for two equation-system in asymptotic variables,

$$\boldsymbol{u} = \frac{1}{c}\begin{bmatrix}\delta^* \\ \varepsilon\end{bmatrix}, \tag{2-10a}$$

$$\boldsymbol{f}^t(\boldsymbol{u}) = \begin{bmatrix}-u_e & 0 \\ 0 & -q_e^2\end{bmatrix}\boldsymbol{u}, \tag{2-10b}$$

$$\boldsymbol{f}^x(\boldsymbol{u}) = \begin{bmatrix}u_e(2B'_u q_e - u_e) & -B'_u q_e^2 \\ q_e^2 H_k(2B'_u q_e - u_e) & -q_e^2 H_k \frac{q_e}{u_e} B'_u q_e\end{bmatrix}\boldsymbol{u} + \frac{q_e^2}{c}\begin{bmatrix}\frac{1}{2}(p^* + p') \\ \frac{\dot{m}}{\delta_\psi}(p^* + p')\end{bmatrix}, \tag{2-10c}$$

$$\boldsymbol{s}(\boldsymbol{u}) = \begin{bmatrix}u_e\partial_x u_e & 0 \\ -\partial_t q_e^2 & 0\end{bmatrix}\boldsymbol{u} - \frac{1}{c}\begin{bmatrix}R_z\delta_\psi + \frac{1}{2}C_f \\ 2\mathrm{Re}_\delta^{-1}\mathcal{D}u_e^3\end{bmatrix}, \tag{2-10d}$$

where $R_z = \frac{1}{2}\partial_x u_z^2 + \frac{u_z}{u_e}\partial_t u_z$.

Each term given above is denoted as follows: B $(-)$ is the boundary layer budget factor, H $(-)$ is the boundary layer shape factor, H_k $(-)$ is the kinetic energy shape factor, p^* (m) is the pressure incremental thickness, δ_ψ (m) is the streamline-to-surface distance, δ^* (m) is the displacement thickness, δ_k (m) is the kinetic energy thickness, ϵ (m) is the mechanical energy thickness, θ (m) is the momentum thickness, ρ (kg/m^3) is the fluid density, $\boldsymbol{u}$ (m/s) is the fluid velocity, p (kg/ms^2) is the pressure, τ (kg/ms^2) is the stress , μ (kg/ms) is the dynamic viscosity, ν (m^2/s) is the kinematic viscosity, Φ (kgm^2/s^3) is the dissipation, and q_e and u_e are the nondimensionalized magnitudes of the total and $x-$component edge velocities, respectively, normalized with respect to the undisturbed velocity which is assumed to be at infinity as follows:

$$u_e = \frac{U_e}{U_\infty} \qquad \text{and} \qquad q_e = \frac{Q_e}{Q_\infty}$$

The definitions are given as below. The tilde denotes the curvature effects.

Asymptotic integral quantities
(all with dimension of distance):

$$\tilde{\delta}^* \overset{\text{def}}{=} \int_0^{\delta_\psi} \left(1 - \frac{u}{U_e}\right) \mathrm{d}\tilde{y},$$
$$\theta \overset{\text{def}}{=} \int_0^{\delta_\psi} \frac{u}{U_e}\left(1 - \frac{u}{U_e}\right) \mathrm{d}y,$$
$$p^* \overset{\text{def}}{=} \int_0^{\delta_\psi} \left(1 - 2\frac{p_0 - p}{\rho Q_e^2}\right) \mathrm{d}y,$$
$$\tilde{\varepsilon}_k \overset{\text{def}}{=} \int_0^{\delta_\psi} \left(1 - \frac{\boldsymbol{u}\cdot\boldsymbol{u}}{Q_e^2}\right) \mathrm{d}\tilde{y},$$
$$\delta_k \overset{\text{def}}{=} \int_0^{\delta_\psi} \frac{u}{U_e}\left(1 - \frac{\boldsymbol{u}\cdot\boldsymbol{u}}{Q_e^2}\right) \mathrm{d}y$$

Conserved integral quantities
(mass, momentum and energy):

$$\delta_\psi \overset{\text{def}}{=} \text{‘Orthogonal distance from the wall to a streamline or stream surface’}$$
$$\dot{m} \overset{\text{def}}{=} \frac{1}{\rho U_\infty}\int_0^{\delta_\psi} \rho u \mathrm{d}\tilde{y} = u_e(\delta_\psi - \tilde{\delta}^*),$$
$$\tilde{e}_k \overset{\text{def}}{=} \frac{1}{\rho U_\infty^2}\int_0^{\delta_\psi} \rho \boldsymbol{u}\cdot\boldsymbol{u} \mathrm{d}\tilde{y} = q_e^2(\delta_\psi - \tilde{\varepsilon}_u)$$

Nondimensional factors:

Classical

$$H \overset{\text{def}}{=} \delta^*/\theta\ ,$$
$$H_k \overset{\text{def}}{=} \delta_k/\theta$$
$$\lambda \overset{\text{def}}{=} \frac{\theta^2}{\nu}\frac{\partial U_e}{\partial x} \text{ (Holstein-Bohlen)}$$
$$F \overset{\text{def}}{=} \frac{U_e}{\nu}\frac{\partial \theta^2}{\partial x} \text{ (Thwaites)}$$
$$S \overset{\text{def}}{=} \frac{\tau_w \theta}{\mu U_e} = \frac{u_\tau^2}{u_e^2}\mathrm{Re}_\theta$$

Conservative

$$B_u = \frac{U_e^2}{Q_e^2}\frac{\delta_\psi - \delta^* - \theta}{\delta_\psi - \varepsilon_k},$$
$$\mathcal{D} \overset{\text{def}}{=} \frac{\mathrm{Re}_\delta}{\rho U_e^3}\int_0^{\delta_\psi} \Phi \mathrm{d}\tilde{y},$$

In the rest of this thesis, above set of equations (2-10) is used as the governing equation of the viscous region.

Chapter 3

Flow model in inviscid region

Because the effects of viscosity are limited to a very thin layer near to the body (*the boundary layer*) and also to the wake region, they can be discarded from the model. In this manner, the governing equations for the inviscid flow become considerably simpler. In addition to discarding viscosity, even further approximations can be made leading to a potential flow model, where solving the Laplace equation instead of the full Navier-Stokes equations is sufficient.

The realization behind this simplification can be explained by observing a fluid particle moving along its path l. Within the concept of continuum mechanics, the most prominent effect of viscous forces on the flow is the distorting the fluid particles. In other words, when the viscous forces are very large, the fluid particle will rotate as a rigid body and follow the path l illustrated in Figure 3-1 whereas for negligible viscosity, having no shear force effect, the fluid particle may not rotate. In this case, flow is considered to be *irrotational flow*.

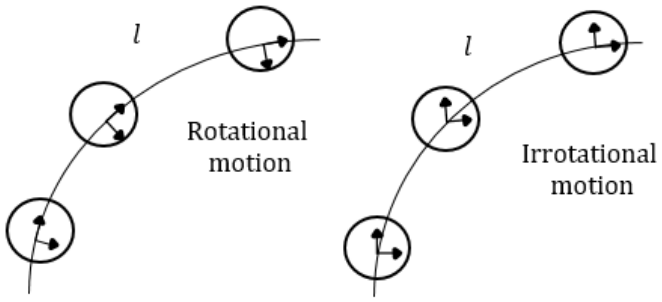

Figure 3-1: *Rotational and irrotational motion of a fluid particle.*

Considering the line integral along the line C on the path l, the velocity vector $\boldsymbol{q}$, integrated over C can be expressed as

$$\int_C \boldsymbol{q} \cdot dl = \int_C udx + vdy. \tag{3-1}$$

As a consequence of irrotational flow, $udx + vdy$ becomes an exact differential of a potential Φ that is independent of the integration path C and is a function of the location of the point $P(x, y)$

$$\Phi(x, y) = \int_{P_0}^{P} udx + vdy \tag{3-2}$$

where P_0 is an arbitrary reference point. Φ represents the velocity potential and the velocity field can be obtained as its gradient

$$\boldsymbol{q} = \nabla\Phi \tag{3-3}$$

and in Cartesian coordinates

$$u = \frac{\partial\Phi}{\partial x} \quad v = \frac{\partial\Phi}{\partial y}. \tag{3-4}$$

Substitution of (3-3) into the continuity equation yields

$$\nabla \cdot \boldsymbol{q} = \nabla \cdot \nabla\Phi = \nabla^2\Phi = 0. \tag{3-5}$$

This equation, (3-5), is the *Laplace equation.* It is a linear elliptic partial differential equation governing the behaviour of the velocity for an inviscid, incompressible, and irrotational flow. Due to its ellipticity, in order to solve it, the boundary conditions are needed to be prescribed on all solid surfaces and at infinity. However, having neglected the viscosity of the fluid prohibits the no-slip boundary condition to be specified on a solid-fluid interface. On the other hand, the normal component of the relative velocity between fluid and the solid surface (which may have a velocity $\boldsymbol{q}_B$) can be stated as zero at the boundary

$$\boldsymbol{n} \cdot (\boldsymbol{q} - \boldsymbol{q}_B) = 0, \tag{3-6}$$

where n is the unit vector in normal direction.

Summarizing what has been done until here, splitting the domain into two parts and considering the mathematical problem of the inviscid one, where viscosity is negligible, the problem is reduced to solving the Laplace equation to obtain the velocity field created, say, by the

motion around an airfoil or a wing with suitable boundary conditions specified on the body and at infinity. In a space-fixed reference frame, this mathematical problem can be stated as:

$$\nabla^2\Phi = 0 \tag{3-7a}$$

$$\frac{\partial\Phi}{\partial\boldsymbol{n}} = \boldsymbol{n}\cdot\boldsymbol{q}_B \quad on\ body\ surface \tag{3-7b}$$

$$\nabla\Phi \to 0 \quad at \quad r\to\infty. \tag{3-7c}$$

The above set of equations (3-7) is called the *Neumann exterior problem* because the Neumann boundary condition is specified on the body surface and the flow is considered in the region exterior to the body. On the other hand, if instead of specifying the normal derivative of the potential on the boundary (3-7b), a constant value of Φ is prescribed on the surface, in other words the potential is specified on the solid surfaces, then above set of equations, (3-7), comprise the *Dirichlet exterior problem*. Note that although the model describes unsteady, irrotational inviscid flow, the mathematical formulation leads to a boundary value problem, not an initial value problem. As will be discussed later, this means that the unsteady effects are not present in the partial differential equation, but it is introduced via boundary conditions. The effect of the geometry submerged in the flow manifests itself through the boundary conditions. However, this does not mean that every geometry may have its unique formulation. As the mathematical problem of potential flow is linear, a linear combination of elementary solutions can be found that satisfies the set of geometrical boundary conditions. This can be done by distributing the singularity elements (elementary solutions) - the strength of which have to be determined as a part of the solution procedure as will be represented in following sections. In this manner, the induced velocities resulting from the elementary solutions that satisfy the irrotationality condition and the boundary layer at infinity can be calculated.

A great amount of publications can be found concerning the potential flow theory. In this section, for the discussion of the potential flow as well as the panel method, Katz and Plotkin [33] and Van Garrel [34] are taken as the main reference. In addition to these two references, an extensive explanation of the details of the panel method can be found in [35].

In the case of viscous-inviscid interaction, a new concept called the transpiration velocity is introduced in order to take the effect of viscosity on the potential flow into consideration. It was derived by Lighthill [36] and following it, there are a great number of publications where transpiration velocity has been seen (e.g. Balleur [37], Bartels [38]). The unsteady form of the transpiration velocity is derived more recently using an asymptotic approach by Bartels [39]. Furthermore, Cebeci *et al* [15] developed an unsteady panel method in a similar fashion with the one employed here developed by Van Garrel [40].

3-1 Mathematical Model

The potential flow problem is formulated as an elliptic second order partial differential equation with the appropriate boundary conditions. In this section, these boundary conditions are introduced for an arbitrary geometry which yields the general solution of (3-7). A geometrical representation of the problem is given below.

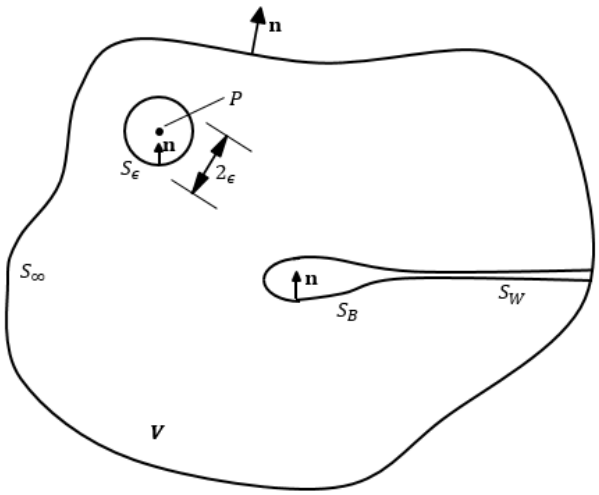

Figure 3-2: *Nomenclature used to define potential flow problem*

In Figure 3-2, three boundaries can be observed: the boundary of an arbitrary body S_B, the outer boundary S_∞, and the wake boundary S_W. All these boundaries are enclosed in a volume V and they will be specified by the boundary conditions, expressed as (3-7b) and (3-7c) in accordance with either Dirichlet or Neumann formulation. The whole set of equations (3-7), is solved for the velocity potential. The normal vector $\boldsymbol{n}$ is defined to point into the exterior of the domain of interest. It is of great importance to note that (3-7) shows no explicit time-dependence whereas the velocity potential $\Phi(\boldsymbol{x}, t)$ does depend on both space and time. Unsteady effects enter the problem through the boundary conditions. Therefore, during the derivations, this time-dependency is implicitly assumed.

Equation (3-7) can be restated through Green's second identity which is derived from application of the divergence theorem to the vector field $F = \Phi_1 \nabla \Phi_2 - \Phi_2 \nabla \Phi_1$ where Φ_1 and Φ_2 are two twice continuously differentiable scalar functions. This results in

$$\int_S (\Phi_1 \nabla \Phi_2 - \Phi_2 \nabla \Phi_1) \cdot dS = \int_V (\Phi_1 \nabla^2 \Phi_2 - \Phi_2 \nabla^2 \Phi_1) dV, \tag{3-8}$$

where S corresponds to all boundaries, including the wake boundary S_W:

$$S = S_B + S_W + S_\infty. \tag{3-9}$$

For the two dimensional case, scalar functions are defined as

$$\Phi_1 := \ln r \quad and \quad \Phi_2 := \Phi, \tag{3-10}$$

where Φ is the velocity potential function in point P inside V and r is the distance from an arbitrary fixed point $P(x, y)$ to a point $Q(x, y)$ on the enclosing surface, then $\boldsymbol{r} = P - Q$ and $r = |\boldsymbol{r}|$.

Notice that Φ_1 approaches minus infinity as r approaches to zero which makes it singular. This term is the potential induced by an elementary solution defined as a source.

In order to obtain a general solution, different locations of the point P, inside or outside V, are considered.

In the first case, the point P is placed outside V. Then, both Φ_1 and Φ_2 satisfy Laplace equation and (3-8) becomes

$$\int_S (\ln r \nabla\Phi - \Phi\nabla \ln r) \cdot \boldsymbol{n}\, dS = 0. \tag{3-11}$$

The second case, also of particular interest, is when the point P is placed inside the region V as given in Figure 3-2. In order to exclude the point P from the region of integration, a small circle with radius ϵ is introduced. Outside of the circle and in the remaining region V, again, both Φ_1 and Φ_2 satisfy the Laplace equation and (3-8) becomes

$$\int_{S+circle\,\epsilon} (\ln r \nabla\Phi - \Phi\nabla \ln r) \cdot \boldsymbol{n}\, dS = 0. \tag{3-12}$$

Having evaluated the outer region, the part of the integral over the circle should be elaborated. To begin with, a local polar coordinate system at P is introduced; the vector $\boldsymbol{n}$ points inside the small circle, $\boldsymbol{n} = -\boldsymbol{e_r}$ then following expressions can be obtained for the normal derivative for the potential and the gradient of the potential on the boundary

$$\boldsymbol{n} \cdot \nabla\Phi = -\frac{\partial\Phi}{\partial r} \quad \text{and} \quad \nabla(\ln r) = -\left(\frac{1}{r}\right)\boldsymbol{e_r}. \tag{3-13}$$

Substitution of (3-13) into (3-12) yields

$$-\int_{circle\,\epsilon} \left(\ln r \frac{\partial\Phi}{\partial r} - \frac{\Phi}{r}\right) dS + \int_S (\ln r \nabla\Phi - \Phi\nabla \ln r) \cdot \boldsymbol{n}\, dS = 0. \tag{3-14}$$

Considering the circle with a radius of ϵ, $\int dS = 2\pi\epsilon$. Taking the limit for $\epsilon \to 0$ (assuming that the potential and its derivatives are well-behaved functions) the first term in the first integral of (3-14) vanishes, while the second term becomes

$$\int_{circle\,\epsilon} \left(\frac{\Phi}{r}\right) dS = 2\pi\Phi(P). \tag{3-15}$$

Then, (3-14) can be written as

$$\Phi(P) = -\frac{1}{2\pi}\int_S (\ln r \nabla\Phi - \Phi\nabla \ln r)\cdot \boldsymbol{n}\, dS. \tag{3-16}$$

This formula gives the velocity potential for an arbitrary point P in the flow, inside the region V.

The third case occurs when the point of interest P is placed on the boundary S_B. After the same procedure is applied, but considering a semicircle instead of a full circle, the result is

$$\Phi(P) = -\frac{1}{\pi}\int_S (\ln r \nabla\Phi - \Phi\nabla \ln r)\cdot \boldsymbol{n}\, dS. \tag{3-17}$$

Point P is placed everywhere except one region, which brings the final case, where the point P lies inside the boundary of S_B which causes an internal potential Φ_i. Considering this point P which is exterior to S_B and applying (3-16) yields

$$0 = -\frac{1}{2\pi}\int_S (\ln r \nabla\Phi_i - \Phi_i\nabla \ln r)\cdot \boldsymbol{n}\, dS. \tag{3-18}$$

The direction vector $\boldsymbol{n}$ points outward from S_B. In order to obtain a form that takes the influence of the inner potential into consideration as well, (3-16) is added to (3-18) which yields

$$\Phi(P) = -\frac{1}{2\pi}\int_{S_B} (\ln r \nabla(\Phi-\Phi_i) - (\Phi-\Phi_i)\nabla \ln r)\cdot \boldsymbol{n}\, dS - \frac{1}{2\pi}\int_{S_\infty+S_W} (\ln r \nabla\Phi - \Phi\nabla \ln r)\cdot \boldsymbol{n}\, dS, \tag{3-19}$$

where the inner potential is considered to be in the opposite direction of $\boldsymbol{n}$. The second integral contains the contribution of the singularity distribution on S_∞ (when it is considered to be far from S_B) which may be defined as

$$\Phi_{S_\infty} = -\frac{1}{2\pi}\int_S (\ln r \nabla\Phi - \Phi\nabla \ln r)\cdot \boldsymbol{n}\, dS. \tag{3-20}$$

The potential of the outer surface depends on the selection of the coordinate system. If there is no body motion, it can be selected as a constant in this region. Having defined the potential on the surfaces S_B and S_∞, what remains is an equation for the wake region. If it is assumed to be thin, such that $\partial\Phi/\partial n$ remains continuous, (3-19) becomes

$$\Phi(P) = -\frac{1}{2\pi}\int_{S_B} (\ln r\, \nabla(\Phi-\Phi_i) - (\Phi-\Phi_i)\nabla \ln r)\cdot \boldsymbol{n}\, dS - \frac{1}{2\pi}\int_{S_W} \Phi\, \boldsymbol{n}\cdot\nabla \ln r\, dS + \Phi_\infty(P). \tag{3-21}$$

Having emphasized earlier that the Laplace equation and the necessary boundary conditions together constitute a boundary value problem, it can be easily noticed that all potential equations (3-16), (3-19), and (3-21) provide the value of $\Phi(P)$ in terms of Φ and $\partial\Phi/\partial n$ on the boundaries. Hence, in order to obtain the solution, these values on the boundaries have to be determined.

The potential equations (3-16), (3-19), and (3-21) can be simplified using the following definitions:

$$-\mu := (\Phi - \Phi_i) \tag{3-22}$$

$$\sigma := \nabla(\Phi - \Phi_i) \cdot \boldsymbol{n}. \tag{3-23}$$

These elements are called the doublet (μ) and the source (σ) distributions and correspond to the surface singularity strength. In addition, since the flow is unsteady, they depend both on time and location. They will act like elementary solutions. Using the definitions (3-22) and (3-23), (3-19), replacing $\boldsymbol{n} \cdot \nabla$ by $\partial/\partial n$, can be written as

$$\Phi(P) = -\frac{1}{2\pi}\int_{S_B} \sigma \, \ln r \, dS - \frac{1}{2\pi}\int_{S_B+S_W} \mu \frac{\partial}{\partial n} \ln r \, dS + \Phi_\infty(P). \tag{3-24}$$

The problem (3-7) is now reduced to solving the following equation:

$$\Phi = \varphi_\mu + \varphi_\sigma + \Phi_\infty, \tag{3-25}$$

where φ_μ and φ_σ are perturbation velocity potentials contributed by doublet and source singularity distributions on the inner boundaries, respectively, given as

$$\varphi_\mu = -\frac{1}{2\pi}\int_{S_B+S_W} (\mu \nabla \ln r) \cdot \boldsymbol{n} \, dS, \tag{3-26}$$

$$\varphi_\sigma = -\frac{1}{2\pi}\int_{S_B} (\ln r \, \sigma) \cdot \boldsymbol{n} \, dS, \tag{3-27}$$

and Φ_∞ is the unperturbed reference velocity potential when no boundaries are present. The effect of the potential induced by the singularity distribution on the wake has to be considered separately. This treatment is explained in the following sections.

Unsteady formulation of potential flow model

Note that the above equations have been derived without taking into account the unsteady effects of the system. However, as stated before, the time-dependency is considered implicitly throughout the derivation since it is embedded in the system via the boundary conditions. This means the whole derivation to obtain a boundary value problem for the velocity potential

Φ at a point P can be *extended* as a function of time taking into account that the singularity distribution is updated continuously at every instant of time. Therefore, the time dependent solution of the potential flow problem (3-7) can be given as:

$$\Phi(P,t) = \varphi_\mu(P,t) + \varphi_\sigma(P,t) + \Phi_\infty(P,t), \tag{3-28a}$$

$$\varphi_\mu(P,t) = -\frac{1}{2\pi}\int_{S_B+S_W} (\mu \nabla \ln r)\cdot \boldsymbol{n}\, dS, \tag{3-28b}$$

$$\varphi_\sigma(P,t) = -\frac{1}{2\pi}\int_{S_B} (\ln r\, \sigma)\cdot \boldsymbol{n}\, dS, \tag{3-28c}$$

where the distance between evaluation point and boundary may also depend on time, then $\boldsymbol{r} = \boldsymbol{r}(t)$.

The velocity potential can be determined from (3-28) provided that the appropriate singularity distribution over the boundary is determined in such a way that the boundary conditions (3-7b) and (3-7c) are satisfied. Hence the task is, now, finding these distributions. Also note that the appropriate singularity distributions, i.e. the combination of the sources and doublets for a particular problem, depend on the geometry of the problem.

3-1-1 Boundary conditions

As already stated in the preceding sections, the potential flow problem (3-7) can be formulated as either a Neumann or a Dirichlet problem. Within the framework of this thesis, external Dirichlet boundary conditions are chosen because the interest is kept in the flow field on one side of the surface with already *prescribed* values. In the Dirichlet formulation, the potential inside the body surface Φ_i is specified as a constant value and this value is prescribed on all the solid surfaces. Then, the solution is extended to the wake region.

The exterior and interior implies the regions of the flow illustrated in Figure 3-3.

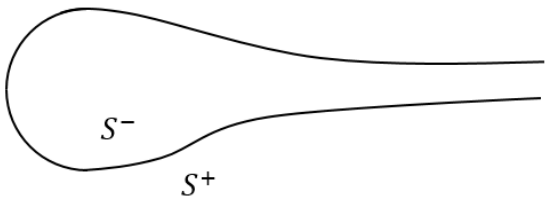

Figure 3-3: *The exterior and interior regions.*

The first one is, represented by S^+, the inviscid flow where the Laplace equations needs to be solved. The other region, represented by S^-, has no physical meaning, represents a fictitious flow with a known velocity potential prescribed by Dirichlet condition:

$$\Phi_i = \Phi(P,t). \tag{3-29}$$

Separating the region of interest into S^+ and S^-, since its integrand is singular, the perturbation velocity potential due to doublet distribution (3-28b) causes a jump in the velocity potential of strength $\mu(P,t)$ across the surface:

$$\varphi(P \to S^{\pm}, t) = \varphi_{\sigma}^{P}(P,t) + \varphi_{\mu}^{P}(P,t) \pm \frac{1}{2}\mu(P,t). \tag{3-30}$$

The two $\varphi^P(P,t)$ terms on the right hand side of (3-30) can be interpreted as Cauchy Principal Value or Finite Part integrals over the whole solid surfaces around the body, excluding an infinitesimal region around the singular point from the surface of integration. Hence, the separation of the surface does not cause a mathematical problem.

With the velocity potential known (3-29), the velocity field can be expressed as

$$\boldsymbol{q}_i(P,t) = \nabla\Phi_i. \tag{3-31}$$

The velocity at the surface is expressed by the boundary condition at the surface side S^+ as the sum of the normal component of the surface velocity $\boldsymbol{q_s}(P,t)$, plus a specified velocity $v_n(P,t)$ in the normal direction:

$$\nabla\Phi \cdot \boldsymbol{n} = \boldsymbol{q_s} \cdot \boldsymbol{n} + v_n, \qquad P \to S^+ \tag{3-32}$$

The normal velocity distribution is an additional term which can be used to take for example the boundary layer displacement thickness effect into consideration. The local surface velocity term, on the other hand, can be arisen from the shear stress effects on the boundary like surface rate of deformation, surface translation *etc.*

Recall that in order to solve (3-28), the source and doublet distributions, σ and μ, need to be determined.

First, the source strength σ can be determined by substituting (3-32) into the definition of the source strength (3-23), which yields:

$$\sigma(Q,t) = (\boldsymbol{q_s} - \boldsymbol{q_i}) \cdot \boldsymbol{n} + v_n, \qquad Q \in S. \tag{3-33}$$

Having defined the source strength, the doublet strength demands attention. Boundary integral equation (3-28a) is rearranged for the point P inside the body approaching the surface S^-

$$\varphi_{\mu}(P,t) = \Phi_i(P,t) - \varphi_{\sigma}(P,t) - \Phi_{\infty}(P,t), \qquad P \to S^-. \tag{3-34}$$

After the source distribution has been determined form (3-33), the doublet strength can be solved from (3-34).

The normal component of the velocity at the surface side of interest S^+ is expressed in (3-32). The tangential component of the the velocity, on the other hand, can be expressed by taking the surface gradient of doublet strength (3-23) which yields

$$\nabla_s \Phi(P,t) = \nabla_s \Phi_i - \nabla_s \mu, \qquad P \to S^+. \tag{3-35}$$

Now, combining normal and tangential component of the velocity with source strength (3-33), gives an expression for the velocity at the surface in terms of the known velocity field and the perturbation flow field resulting from the source and doublet singularity distributions:

$$\boldsymbol{q}(P,t) = \boldsymbol{q_i} + \sigma \boldsymbol{n} - \nabla_s \mu. \tag{3-36}$$

Here, the final solution is expressed in terms of the inner velocity field which corresponds to the non-physical region of the domain S^-. This provides a freedom to choose the terms depending on this non-physical domain, namely $\boldsymbol{q_i}$, which also means choosing the velocity potential inside the body surface Φ_i. A general approximation is to choose $\Phi_i = \phi_i + \Phi_\infty$ and since the internal perturbation potential ϕ_i is set to zero, the velocity potential inside the body can be reduced to Φ_∞ which also means that $\boldsymbol{q_i} = \boldsymbol{q_\infty}$. Then assuming a known surface velocity $\boldsymbol{q_s}$ and the normal velocity v_n, the velocity distribution can be determined from the following set of equations:

$$\sigma = (\boldsymbol{q_s} - \boldsymbol{q_\infty}) \cdot \boldsymbol{n} + v_n \boldsymbol{n}, \tag{3-37a}$$

$$\varphi_\mu = -\varphi_\sigma, \tag{3-37b}$$

$$\boldsymbol{q}(P,t) = \boldsymbol{q_\infty} + \sigma \boldsymbol{n} - \nabla_s \mu. \tag{3-37c}$$

The above set of equation (3-37a) - (3-37c) defines the mathematical model for the flow in the inviscid region. The first equation (3-37a) implies that the source strength is adjusted to give zero normal velocity over the body and (3-37b) implies that the doublet strength is acting upon the changes on the source strength. But notice that the boundary S_W in (3-28b) indicates that the doublet strength is not only dependent on the source strength specified on the body but also it reacts to the changes along the wake region. Hence, the doublet strength needs to be determined on the wake region as well. In order to ensure a unique solution, the Kutta condition is imposed to take wake effect on the doublet into account.

Kutta Condition

The wind turbine blades are manufactured using the certain airfoil families and these airfoils are designed in such a way that they facilitate to produce lift in order to rotate the blades by creating a pressure difference between the upper and lower sides of the airfoil which causes a circulation. This circulation can be manipulated into different forms of vortex shedding behind the airfoil by using the different trailing edge configurations. Therefore, the modelling of the wake region is very important for accurate prediction of the lift produced by the airfoil.

The Kutta condition [33] adjusts the doublet strength to satisfy the conditions associated with the circulation created around the airfoil.

While it is possible to specify the source strength for a general solution in a straightforward approach, the doublet strength distribution involves physical phenomena that require additional conditions to be imposed to arrive to a unique solution. The Kutta condition has been defined to take wake effects into consideration by uniquely relating the doublet strength in the wake to the doublet strength at the trailing edge. In its most general form, the Kutta condition requires that the velocity at the trailing edge is bounded

$$|\nabla \Phi_{te}| < \infty. \tag{3-38}$$

The objective here is to express the doublet strength in the wake in terms of the strength at the trailing edge to be able to determine the potential in the wake. Considering the most basic approach, along the thickness of wake, this potential can be expressed as the difference between the potential values at the upper and lower surface at the trailing edges.

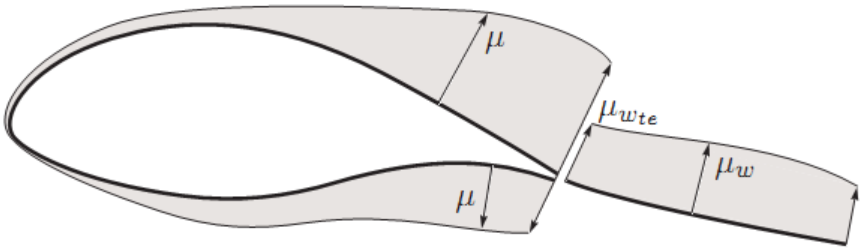

Figure 3-4: *Kutta condition around trailing edge [34].*

This relation may be formulated as follows

$$\mu_{w_{te}} = \mu_{te_u} - \mu_{te_l}. \tag{3-39}$$

In unsteady flows, the Helmholtz theorem of conservation of vorticity (which is also stated as Kelvin's theorem) provides an additional equation for the evolution of the wake that can be employed to determine the streamwise strength of the vorticity shed into the wake. Helmholtz stated that the time rate of change of circulation around a closed curve consisting of the same fluid elements is zero. It can be formulated as

$$\frac{d\Gamma}{dt} = 0 \qquad \text{for any t,} \tag{3-40}$$

where the Γ is the circulation around a fluid curve enclosing the body and its wake. This statement implies that for each time instant the overall circulation must be conserved keeping the vorticity around the airfoil constant.

Utilizing the Helmholtz's theorem brings the need of the vorticity formulation of the general equations for the fluid motion in the case of incompressible, unsteady, inviscid flow which can be obtained by applying the curl operator to the momentum conservation equation which after some manipulations yields [33]:

$$\frac{D\boldsymbol{\omega}}{Dt} = \boldsymbol{\omega} \cdot \nabla \boldsymbol{q}. \tag{3-41}$$

Then, the circulation Γ may be expressed as (using Stokes theorem)

$$\Gamma = \iint_S \boldsymbol{\omega} \cdot \boldsymbol{n}\, dS = \int_{\partial S} \boldsymbol{q} \cdot \bar{\tau}\, ds, \tag{3-42}$$

where $\boldsymbol{n}$ is the unit normal vector to the cross section surface S, and $\bar{\tau}$ is the unit vector tangential to the contour ∂S.

It can now be concluded that given the initial characteristics of the flow at time t_0, these characteristics shall be preserved along the whole wake which may be formulated in terms of the wake element $\boldsymbol{X_w}$ and the wake doublet strength μ_w as follows:

$$\frac{d\boldsymbol{X_w}}{dt} = \boldsymbol{q} \qquad \boldsymbol{X_\mu}(t_0) = x_{te}(t_0), \tag{3-43a}$$

$$\frac{D\mu_w}{Dt} = 0 \qquad \mu_w(t_0) = \mu_{w_{te}}(t_0). \tag{3-43b}$$

The unsteady wake effect is implemented in the panel method based on the potential solver developed by Van Garrel. The related PhD work about this tool has not yet been publish [40]. Furthermore, the justification of this approach is discussed in the last chapter.

Solution of inviscid flow problem

The problem (3-7) is reduced to finding the appropriate source and doublet distributions on the surface of the body (S_B, S_W) which automatically fulfill the boundary condition (3-7c) by having velocity fields that decay as $\boldsymbol{r} \to \infty$ whereas becoming singular when $\boldsymbol{r} = 0$. Each of these singularities is basic solutions and by integrating them over the body surface, the general solution can be obtained. This formulation is given in (3-28).

One last consideration is the presence of the boundary layer. Notice that the whole solution procedure is valid only under the assumption of inviscid flow. However, in the scope of this thesis VII coupling is of primary concern. Thus, the presence of the boundary layer and its influence on the potential flow is taken into consideration and a *modification* is introduced whereby the solution of the whole flow field becomes concordant with the Navier-Stokes equations. Hence, a concept, namely, *viscous potential flow* is introduced [2].

3-2 Effect of the boundary layer on potential flow

The potential flow problem as it is described in the preceding sections has ignored the presence of the boundary layer and as the reduced system indicates, the solution is obtained by means of finding the appropriate elementary solutions on the surface of the body. However, the flow around the body develops a boundary layer which displaces the inviscid region a distance equal to the boundary layer thickness. This means that the body becomes thicker then it actually is and the inviscid flow develops starting from this thickness considering it as the new stream surface. This new physical geometry is called the *effective displacement body* which corresponds to the actual physical body plus the displacement thickness. The effect of this displacement can be imagined as to *calibrate* the no-slip condition, i.e. normal component of the velocity on the body is zero, to *catch* the effect of the boundary layer. This means that the normal velocity component at the surface of the thicker body is set equal to the normal velocity at the edge of the boundary layer. The way to match the normal velocity at the thicker body is done by adding a *transpiration velocity* to the potential equation. The resulting flow is named the *viscous potential flow*.

First, some additional notation is introduced. The total velocity vector is given by $\boldsymbol{q} = (u, v)^T$ where u is the tangential and v is normal velocity component. The velocity at the edge of the boundary layer is indicated with the subscript e.

Using the continuity equation to describe v and assuming v grows linearly with $-(\partial u_e/\partial x)y$, the normal component of the velocity can be approximated inside the boundary layer with the following relation:

$$v(x, y) \approx -\left(\frac{\partial u_e}{\partial x}\right) y + v_n(x) + ..., \qquad y \to \infty, \tag{3-44}$$

where $y \to \infty$ indicates that it approaches to the edge of the boundary layer and v_n corresponds to the transpiration velocity which is expressed in (3-33). The transpiration velocity is now obtained as follows [2]:

$$v_n(x) = \frac{\partial}{\partial x}(q_e \delta^*), \tag{3-45}$$

where $q_e = \sqrt{u_e^2 + v_e^2}$ is the magnitude of the velocity at the edge of the boundary layer.

Bartels [39], on the other hand, derived the following formulation for unsteady case:

$$v_n(x, 0, t) = \frac{1}{\rho}\left(\frac{\partial}{\partial x}(\rho q_e \delta^*) + \frac{\partial}{\partial t}(\rho \delta_R)\right), \tag{3-46}$$

where δ_R is named as the density thickness and for the unsteady but incompressible flow the second term $\frac{\partial}{\partial t}(\rho \delta_R) = 0$ resulting the same expression as (3-45).

Using the transpiration velocity, the displacement thickness is given by

$$\delta^* = \int_0^\delta \frac{1}{\rho_e q_e}(\rho_e u_e - \rho u)dy \tag{3-47}$$

and it corresponds to the rate of change of mass defect.

Next step is to include this transpiration velocity into the potential flow problem. It has been expressed in (3-7c) for the body surface the free-slip boundary condition is given by

$$\nabla\Phi \cdot \boldsymbol{n} = 0. \tag{3-48}$$

However, taking the boundary layer into consideration, this condition is modified to be equal to the transpiration velocity at the edge which corresponds to displace the streamlines outward to include viscous effects:

$$\nabla\Phi \cdot \boldsymbol{n} = v_n(x). \tag{3-49}$$

It has been shown that the presence of the boundary layer affects the source strength by introducing a viscous contribution to the potential flow. Then, the source strength can be split into the sum of the viscous and inviscid contributions:

$$\sigma = \sigma_{inv} + \sigma_{vis}, \tag{3-50}$$

where σ_{vis} is resulting from the presence of boundary layer, namely v_n and σ_{inv} is the Dirichlet condition specified for the inviscid flow. Then, the source distribution on the body surface (3-37a) becomes

$$\sigma = (\boldsymbol{q_s} - \boldsymbol{q_n}) \cdot \boldsymbol{n} + v_n = \sigma_{inv} + \sigma_{vis}. \tag{3-51}$$

Taking the effect of the wake into consideration, the equation for the potential including the effect of the boundary layer becomes:

$$\Phi(P,t) = -\frac{1}{2\pi}\int_{S_b} \sigma_{inv} \ln r \, dS - \frac{1}{2\pi}\int_{S_b+S_w} (\mu \boldsymbol{n} \cdot \nabla(\ln r) - \sigma_{vis} \ln r)\, dS + \Phi_\infty(P). \tag{3-52}$$

Then, (3-28b) and (3-28c) takes the following form:

$$\varphi_\mu = -\frac{1}{2\pi}\int_{S_b+S_w} \mu \boldsymbol{n} \cdot \nabla \ln r \, dS, \tag{3-53a}$$

$$\varphi_\sigma = -\frac{1}{2\pi}\int_{S_b} \sigma_{inv} \ln r \, dS - \frac{1}{2\pi}\int_{S_b+S_w} -\sigma_{vis} \ln r \, dS. \tag{3-53b}$$

Following this approach, (3-7) including the boundary layer effect (3-53) can be solved using panel method which is the subject of next section.

3-3 Weak formulation and discretization

Panel methods are one of the first numerical tools developed for routinely analysing the flow around the complex geometries of complete aircraft. They have been widely used and are still being used to solve the inviscid, irrotational flows at subsonic or supersonic Mach numbers mostly in the aerospace and the wind turbine industries due to their ability to provide realistic results for the complex and relatively large flow problems without excessive computational requirements.

In the preceding sections, analytical solutions for the potential flow problem expressed as the source and doublet singularities are obtained whereby the solution of the potential flow problem is reduced to finding the strength of the these singularity elements (elementary solutions) distributed on the boundary surface. Panel methods are based on superimposing the surface distributions of these singularities over small elements, called *panel*s which are chosen to be placed on the boundary of the arbitrary body to make the solution unique.

Panel codes are described as being low-order or high-order. While the former indicates the use of a constant strength singularity distributions over each panel, latter indicates higher order approximations e.g. linear, quadratic, of the distribution over each panel.

Considering the problem in this thesis, the domain is divided into structured grid cells, in other words *panels*, along the body and the wake and a low-order discretization scheme is used. Both the doublet strength and the source strength are specified constant on the panels comprising the surface of the body and the wake. The boundary conditions are imposed on the *collocation points*. The locations of these points can differ according to the panel method implemented.

3-3-1 Discretization of the wing/aerofoil problem

The panel method is applied to find the flow around an airfoil because the main concern in this thesis is analysing the flow around wind turbine blades. The unsteady formulation of the governing equation has been given in (3-37) and the viscous effect is introduced via (3-45). Then the relation between source and doublet strength (3-37b) including the viscous contribution is stated as:

$$\frac{1}{2\pi}\int_{S_b+S_w} \mu \boldsymbol{n}\cdot\nabla \ln r\, dS = -\frac{1}{2\pi}\int_{S_b} \sigma_{inv} \ln r\, dS - \frac{1}{2\pi}\int_{S_b+S_w} -\sigma_{vis} \ln r\, dS. \tag{3-54}$$

Above integrals are calculated by discretizing the wing surface and wake region. Let N_b denotes the number of equal distance segments along the body surface and N_w along the wake. Then the total number of segments is $N = N_b + N_w$.

Recall that using the low-order approach, all singularities are constant and determined by applying the boundary condition at the collocation points of the panels. Each panel, denoted by subscript n has its constant source σ_n and doublet strength μ_n starting from 1 to N. Using the Dirichlet condition for the internal potential, source strength is a given property; the inviscid part is determined from the freestream and the viscous part is known from the

viscous quantities. Then, the only unknown in (3-54) is the doublet strength and the equation can be solved to obtain them by discretizing as follows:

$$\frac{1}{2\pi}\sum_{n-1}^{N_b+N_w}\int_{S_n}\mu\boldsymbol{n}\cdot\nabla\ln r\,dS+\frac{1}{2\pi}\sum_{n-1}^{N_b}\int_{S_n}\sigma_{inv}\ln r\,dS+\frac{1}{2\pi}\sum_{n-1}^{N_b+N_w}\int_{S_n}-\sigma_{vis}\ln r\,dS=0. \tag{3-55}$$

Above (3-55) may be written in the following form where the body collocation points are indexed with $m\in[1,N_b]$:

$$\sum_{n-1}^{N_b+N_w}A_{mn}\mu_n+\sum_{n-1}^{N_b}B_{mn}\sigma_{inv_n}+\sum_{n-1}^{N_b+N_w}B_{mn}\sigma_{vis_n}=0, \tag{3-56}$$

where A_{mn} and B_{mn} are called aerodynamic influence matrices and given by

$$A_{mn}=\int_{S_n}\boldsymbol{n}\cdot\nabla\ln r_{mn}\,dS, \tag{3-57}$$

$$B_{mn}=\int_{S_n}-\ln r_{mn}\,dS. \tag{3-58}$$

A_{mn} and B_{mn} matrices can be regarded as the result of the numerical approximations of the integral expressions for the perturbation velocity potential and components induced by the source and doublet distributions. They represents the influence of the constant source and doublet distribution at panel n on the collocation point m. Note that these matrices are known [33]. Finally, r_{mn} denotes the distance between the pair of collocation points.

Notice that (5-11) is not closed because of the additional unknown doublet distributions on the wake region. The Kutta condition is utilized here to express the unknown doublet strength in the wake using (3-39). Now, the matrix A_{mn} is reduced to a $N_b\times N_b$ matrix and the system is closed for the solution of the doublet strength. For unsteady flow, on the other hand, along the wake more than one panel is needed whose values change with every time step but as stated before, the unsteady effects of the wake region is handled by the panel solver developed by van Garrel and it is not considered in the unsteady scheme developed in this work as described in Chapter 4.

Chapter 4

Viscous-inviscid interaction

Following the revolutionary idea of L. Prandtl [6], the flow field is split into two regions, where the physics of the fluid is governed by completely different equations. However, since these two regions are not independent, this idea introduces a new problem which is not present when the flow field is not split and modelled by the Navier-Stokes equations: How to re-establish the coupling between the viscous and the inviscid region? This coupling is commonly referred to as *viscous-inviscid interaction* (VII).

In the preceding chapters, the governing equations that describe the behaviour of the flow in both regions, the viscous region (the boundary layer) and the inviscid region (the potential flow) are derived. It is important to specify these models in detail because the choice of an optimal VII method clearly depends on the properties of both. In this chapter, the coupling schemes between the viscous and inviscid regions are investigated. In literature, a good review of all VII methods for steady flow can be found by several authors e.g. Le Balleur [37], Lock and Williams [18], and Coenen [2]. For unsteady flows, on the other hand, there are only a limited number of publications concerning the coupling schemes and most of the existing ones are focused on a particular method which is based on the simultaneous solution of the viscous and inviscid models e.g. Drela [1]. The reason behind this is that the physics of the unsteady flows becomes so complicated that to employ an interaction schemes which presume hierarchies cannot provide accurate results. A comprehensive discussion concerning the singularities in the unsteady boundary layers can be found in [41].

In this chapter, a number of different viscous-inviscid interaction schemes are investigated. Different approaches exist to explain the interaction procedure, e.g. the triple-deck theory by Messitier [42] and the functional approach by Brune *et al* [43]. While the triple-deck theory gives an insight into the physics of the problem by dividing the flow field into three layers and consider them individually, the functional approach addresses the matching problem of the simultaneous solution of the non-linear boundary value problems coupled through their boundary conditions. Both approaches give an explanation of the singularity occurring when the skin friction vanishes for the steady laminar flow first shown by Goldstein [23]. For a solid understanding of the coupling mechanisms, both methods are explained keeping the details limited. The reader should refer to the mentioned references for further explanation.

However, it is important to emphasize that, these methods are developed to explain steady boundary layer flows. For unsteady viscous-inviscid interaction, Cebeci denied the existence of a finite-time singularity [44]. However, he was shown to be wrong and a new singularity was introduced by Van Dommelen and Shen [45]. The unsteady boundary layer singularities are also discussed in this chapter. Following the general explanation of the viscous-inviscid interaction, a new unsteady quasi-simultaneous interaction scheme is introduced.

Historical overview

Before the modern technology made large computational power available to solve the full Navier-Stokes equations in the full flow domain, coupling schemes between the boundary layer and inviscid flow were the main approach to obtain a complete flow field solution. Hence, an extensive amount of publications have appeared on this subject over the last hundred years.

The very first idea was based on the mathematical theory of *matched asymptotic expansions* [22]. Here, the flow is solved without considering viscous effects and inviscid velocity distribution is calculated. Then using this distribution, the boundary layer equations are solved which feed the inviscid region with an additional transpiration velocity as a boundary condition resulting in a new velocity distribution. This approach is called *direct method* since it makes use of the *supposed* hierarchy to solve the coupled system sequentially. However, this method fails to provide results when the flow is no longer attached, i.e. when it separates. The reason is the well-known *Goldstein singularity*. In order to resolve this difficulty, Catherall and Mangler [25] developed the *inverse method*. They change the order in the solution sequence of the direct method. However, this method has been shown to converge very slowly. These two methods are referred as *weak* methods since they assume a hierarchy between the two regions and indicate the subsequent exchange of two flow variables.

Following the advances in the mathematical theory of matched asymptotic expansions, Messitier [42] developed the so-called *triple-deck theory* where he successfully showed that the interaction between the inviscid and viscous region can not be simulated as a small correction to the inviscid flow. Both regions have to be considered equally important. This insight naturally leads to so-called *strong* methods where the hierarchy is abolished and both regions are treated of equal importance. The first of these methods that was introduced was the *semi-inverse method* developed by Le Balleur [7] and Carter [46]. It uses the direct method to calculate the inviscid flow and the inverse method to calculate the viscous flow. However, it needs severe relaxation steps which makes it inappropriate for common use. The second one is the *simultaneous method* developed by Lees and Reeves [47]. It calculates both flows simultaneously without any hierarchy, which makes it robust but computationally expensive. And the last important approach is the *quasi-simultaneous method* developed by Veldman [24] where the advantages of the direct and simultaneous method are combined to have a robust solver which has been shown to produce rapidly convergent solutions.

All methods briefly described above are illustrated in Figure 4-1 and will be investigated further in this chapter. However, the main interest is kept in the quasi-simultaneous method since it has been shown to be the most merit candidate for steady flow which rises the question if it is the same case for unsteady flow.

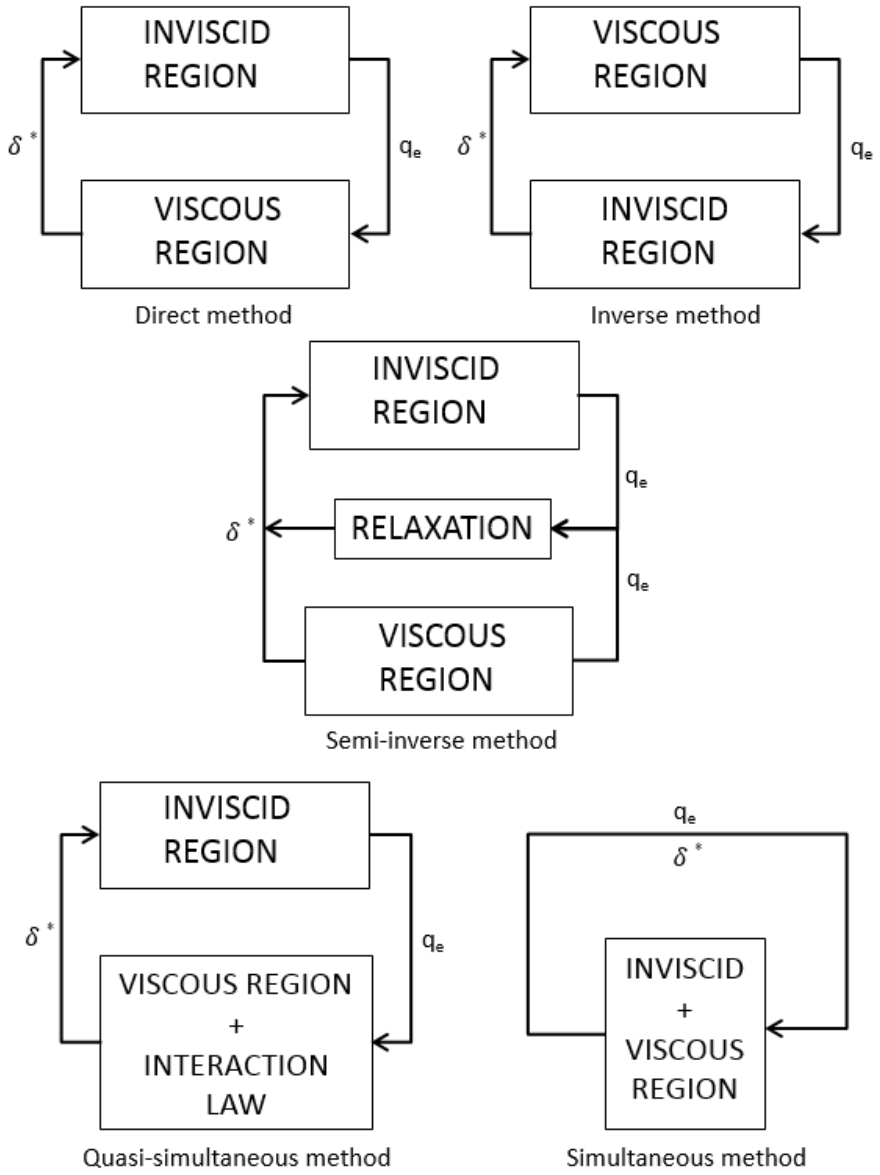

Figure 4-1: *Schematic explanation of the steady interaction methods.*

4-1 Interaction methods

The embodiment behind VII can be briefly summarized as to include the displacement effect caused by the viscosity by means of adding a *transpiration velocity* to the boundary conditions of the potential flow and solve the potential problem by considering this new artificially thickened body. Therefore, it is manifest that the approach employed to couple two regions is through the boundary conditions imposed on each region. The coupling is called *weak* or *strong* depending on the input/output hierarchy of the scheme. The physical interpretation

of the strong and weak coupling, on the other hand, demands additional consideration. Here, two approaches are briefly explained.

Triple-Deck theory

Introduced by Messier [42] and Stewartson [48], Veldman [24] summarized this theory in an abridged fashion. Messier followed an approach based on the asymptotic behaviour of the Navier-Stokes equations. He observed that fixing $x^* = \mathrm{Re}^{\alpha} x/L$, where x/L is the non-dimensional distance from the trailing edge of a flat plate, while taking $\mathrm{Re} \to \infty$, there exists an $\alpha = 3/8$ that corresponds to a distinguished limit where the behaviour of the flow is governed by potential flow theory. Veldman noted that due to the fact that the thickness is only $O(\mathrm{Re}^{-3/8})$, modelling the interaction with the outer flow, a local linearisation will suffice to have a good approximation. This yielded the quasi-simultaneous interaction method which is explained in detail in Section 4.1 and 4.2. Messier investigated if for other values of α alternative approximate equations can be derived. He observed that for $\alpha = -5/8$, the behaviour of the corresponding layer is governed by the boundary layer equations. This layer is called the viscous sublayer. Finally, for $\alpha = -1/2$ he observed that the pressure gradient and the flow deflection are independent. This layer is called the inviscid middle layer. The triple-layered region given schematically in Figure 4-2.

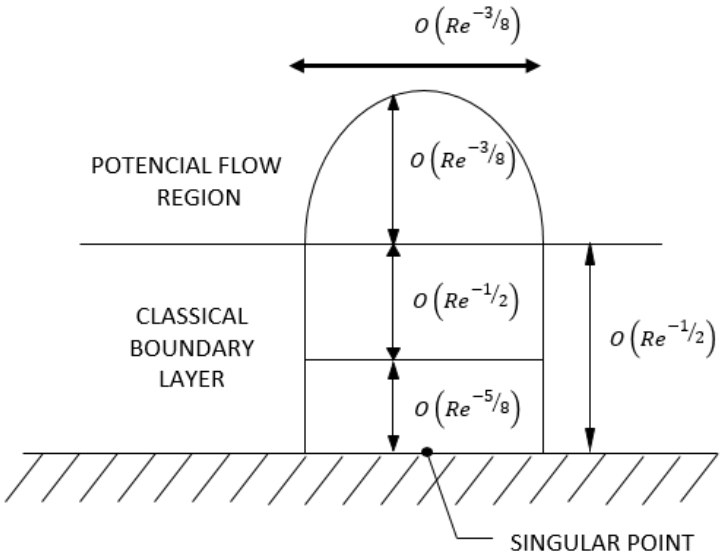

Figure 4-2: *Schematic explanation of the triple-deck theory [24].*

The hierarchy of the problem can be explained considering the asymptotic behaviour for the far upstream and downstream regions in the triple-deck. Veldman observed that, for a laminar, incompressible flow, when $\mathrm{Re}^{3/8}|x| \to \infty$ but $x \to 0$, the pressure is determined by the inviscid flow following the classical boundary layer hierarchy which is modelled by the direct method. However, when $\mathrm{Re}^{3/8} x \to 0$, this hierarchy is inverted and the pressure is determined by the viscous flow which corresponds to the inverse method. This limit behaviour

shows that the interaction between the two regions can never be one-way as is assumed by the direct and the inverse method. The solutions in both the viscous and inviscid region *strongly* depend on each other and any weak formulation will fail to represent the physics of the problem completely, leading to singularities such as Goldstein's [23].

Functional Approach

Introduced by Brune *et al* [43], Williams and Smith [49] extended this approach by giving an explanation of the singularity behaviour of the quasi-simultaneous interaction method.

The main objective here is to obtain a matching solution on the shared surface (the edge of the boundary layer) of the viscous and the inviscid flow that is satisfied simultaneously by both models. Considering the flows separately; first, the solution of the inviscid flow is determined by the displacement thickness that is included in the system via the transpiration velocity given in (3-45) and the shape of the airfoil. The inviscid solution provides the velocity where the boundary layer ends and the inviscid flow starts, called the edge velocity and denoted by q_e. This procedure can be represented in compact form as

$$\boldsymbol{q_e}^P = P\left(\delta^{*^P}\right), \tag{4-1}$$

where superscript P denotes the potential flow. For the boundary layer, on the other hand, the edge velocity determines the displacement thickness:

$$\delta^{*^B} = \hat{B}\left(\boldsymbol{q_e}\right). \tag{4-2}$$

The inverse form of (4-2) is given by:

$$\boldsymbol{q_e}^B = B\left(\delta^{*^B}\right), \tag{4-3}$$

where B stands for the boundary layer region. P and B are the operators which govern the relation between the displacement thickness δ^* and the edge velocity q_e in the viscous and inviscid flow and they are derived using the panel method and the integral boundary layer formulations, respectively.

The matched solution, then, implies that

$$\delta^{*^P} = \delta^{*^B} \qquad \text{and} \qquad \boldsymbol{q_e}^P = \boldsymbol{q_e}^B, \tag{4-4}$$

which is also sketched in Figure 4-3. Note that this is not the case in unsteady flow as is explained in the following sections.

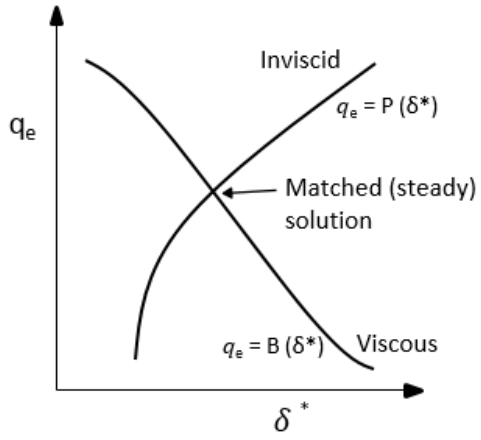

Figure 4-3: *Matched (steady) solution given on the functional view of relationship between viscous and inviscid flows [19].*

Williams and Smith locally linearised (4-1) and (4-3) to examine the features of the different coupling procedures.

For the inviscid flow,

$$\boldsymbol{q_e}^P = P_1 \left(\delta^{*^P}\right) + P_0 \tag{4-5}$$

and for the viscous flow,

$$\boldsymbol{q_e}^B = B_1 \left(\delta^{*^B}\right) + B_0, \tag{4-6}$$

where the value of coefficients matrices P_1, P_0 and B_1, B_0 are known.

In order to give an insight to this functional approach, the direct method and the quasi-simultaneous method are explained briefly.

Figure 4-4 illustrates the coupling procedure of the direct method for the attached and separated flow. It is clear that for the attached flow, the scheme is approaching to the matched solution in each iteration. However, at and beyond the point of separation, this procedure fails. This situation corresponds to the Goldstein singularity for laminar flow.

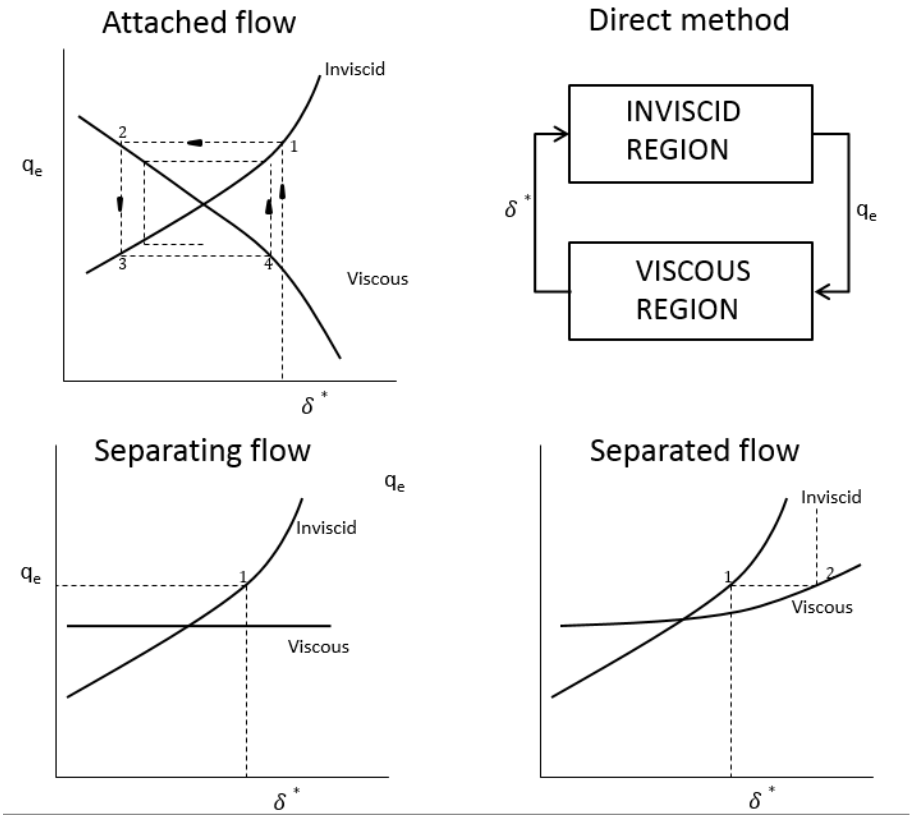

Figure 4-4: *Functional approach of the direct method [19].*

Figure 4-5 illustrates the same coupling procedure as in Figure 4-4 but when the quasi-simultaneous method is applied. As described in detail in the following sections, in the quasi-simultaneous method an approximation to the inviscid flow is derived. Then, it is used as a boundary condition to solve the governing equations of the viscous region (in our case the integral boundary layer equations). This approximation is shown in Figure 4-5 as a linearization (tangent) of the inviscid flow. The intersection of this gives the quasi-simultaneous solution. The procedure continues until the matched solution is reached. It is clear that using this method, it is possible to calculate the solutions even beyond the separation without having to employ inviscid solver multiple times leading to great computational save.

The Triple-Deck and functional approach provide a conceptional understanding of the interaction methods. Now, keeping these approaches in mind, VII methods are introduced following a compact notation:

$$\boldsymbol{q_e} = P\left(\delta^*\right), \tag{4-7}$$

$$\boldsymbol{q_e} = B\left(\delta^*\right), \tag{4-8}$$

where P and B operator are same as given in (4-1) and (4-3) which govern the relation

between the displacement thickness δ^* and the edge velocity $\boldsymbol{q_e}$. The problem here is to find a method that satisfies both (4-7) and (4-8); in other words for given displacement thicknesses obtaining the same velocity distribution along the *edge*. A summary of these methods is given in the beginning of this chapter. Now, they will be investigated in detail.

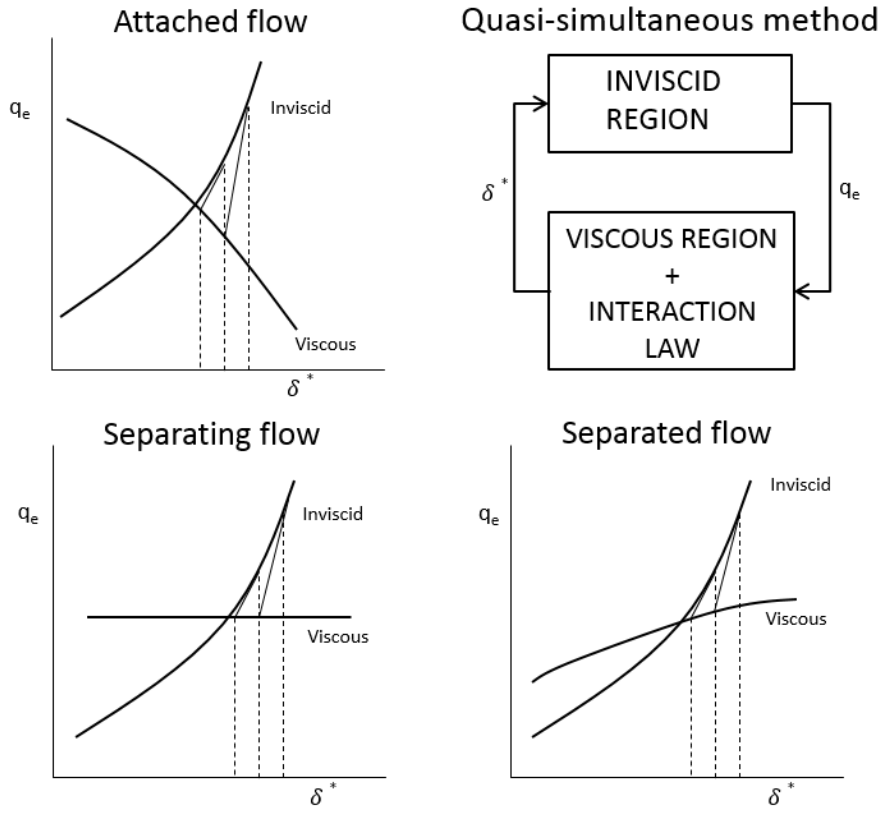

Figure 4-5: *Functional approach of the quasi-simultaneous method [19].*

Direct method

Having the regions separated, the first method that comes to mind is the direct method. The procedure is very intuitive: first, the viscous forces are neglected and considering only potential flow, the velocity vector $\boldsymbol{q_e}$ is calculated. Then, using this velocity vector, the integral boundary layer formulation B is solved which provides the displacement thickness δ^* as a boundary condition for the subsequent solution. The mathematical formulation can be described as:

$$\begin{cases} \boldsymbol{q_e^n} = P\left(\delta^{*^{n-1}}\right), \\ \delta^{*^n} = B^{-1}\left(\boldsymbol{q_e^n}\right) \end{cases} \tag{4-9}$$

where n denotes the number of iterations. This approach is called a weak-interaction method, because of the reasons described in the section discussing the Triple-Deck theory and fails

to provide results when B becomes singular which is known as the Goldstein singularity. Goldstein [23] proved that for steady flow this singularity is observed at the point of vanishing wall shear stress which also corresponds to the separation point as Veldman [26] pointed out. Therefore, the direct method is incapable of coupling beyond separation since the presumed hierarchy between displacement thickness and velocity is no longer valid there.

Inverse method

The inverse method is an attempt to resolve the Goldstein singularity and formulated as the inverse of the direct method. The idea is to prescribe the displacement thickness for the viscous flow as a boundary condition. The mathematical formulation is given as:

$$\begin{cases} \delta^{*^n} = P^{-1}\left(\boldsymbol{q_e^{n-1}}\right), \\ \boldsymbol{q_e^n} = B\left(\delta^{*^n}\right). \end{cases} \tag{4-10}$$

Using this approach Catherall and Mangler [25] were able to overcome the separation problem but still a hierarchy is assumed which means the interaction remains weak. The main drawback of this method is deriving the displacement thickness from the potential flow formulation since it is not known a priori. Furthermore, it needs severe under-relaxation which makes convergence of the solution slow.

Semi-inverse method

This method is introduced by Le Balleur [7] to resolve the problems resulting from assuming a hierarchy between the two regions as mentioned in the description of the direct method, by eliminating the drawbacks of the inverse method. Both the potential flow equations and the boundary layer equations are solved with a prescribed displacement thickness for the velocity distribution. Then, the newly calculated velocity distribution is relaxed with a parameter w to determine the new displacement thickness.

$$\begin{cases} \boldsymbol{q_{e_P}^n} = P\left(\delta^{*^{n-1}}\right), \\ \boldsymbol{q_{e_B}^n} = B\left(\delta^{*^{n-1}}\right), \\ \delta^{*^n} = \delta^{*^{n-1}} + w\left(\boldsymbol{q_{e_P}^n} + \boldsymbol{q_{e_B}^n}\right). \end{cases} \tag{4-11}$$

Notice that in (4-11), while the boundary-layer equations are solved following the inverse method, the potential flow is solved following the direct method. Therefore, no singularity at the point of separation is observed.

Simultaneous method

The simultaneous method implies that both the external flow and the boundary layer equations are solved simultaneously. The mathematical formulation is given as:

$$\begin{cases} \boldsymbol{q_e^n} = P(\delta^{*^n}), \\ \boldsymbol{q_e^n} = B(\delta^{*^n}), \end{cases} \tag{4-12}$$

which yields

$$(B - P)\delta^{*^n} = 0. \tag{4-13}$$

As explained in the discussion of the triple-deck theory, the interaction between the inviscid and viscous flow has a strong character. The simultaneous method takes this strong character into consideration since it introduces no hierarchy between the displacement thickness and the edge velocity. In that way, it also does not show any singularity problem at and beyond the point of separation. However, this method requires intensive computational power. Nishida [12] used this approach to solve steady interacting flow and quite recently Drela [1] published a paper where he solved the unsteady integral boundary layer equations coupled to a panel method, using this simultaneous method.

Quasi-simultaneous method

Among all, the quasi-simultaneous interaction method is of primary importance since it has been shown to be the faster converging and computationally cheaper one. It combines the advantages of the direct and the simultaneous method while successfully avoiding the singularity when the flow separates. The idea behind the quasi-simultaneous method is that the viscous flow equations are solved with an *approximation* of the inviscid flow model as a boundary condition, unlike the direct or inverse method, which is a linear combination of the edge velocity and displacement thickness. Then, subsequently the inviscid flow model is solved. Thus, the singularity problems associated with the weak formulation of the hierarchy are avoided. The mathematical formulation is given as:

$$\begin{cases} \boldsymbol{q_{e_B}^n} - I\left(\delta^{*^n}\right) = \boldsymbol{q_{e_P}^{n-1}} - I\left(\delta^{*^{n-1}}\right), \\ \boldsymbol{q_{e_B}^n} - B\left(\delta^{*^n}\right) = 0, \\ \boldsymbol{q_{e_P}^n} - P\left(\delta^{*^n}\right) = 0, \end{cases} \tag{4-14}$$

where I is called the *interaction law* that provides an approximation of the inviscid flow model. Notice that this interaction law is defined in such a way that it vanishes for the steady interacting problem, in other words it has no effect on the converged solution.

The cardinal point in the quasi-simultaneous method (for steady flow) is to find the best interaction law I which provides rapidly convergent solutions with smallest computational effort. The main form that have been used for the interaction law is the thin-airfoil approximation. It provides a simplified form of the inviscid flow and since for the steady case the influence of the interaction law vanishes anyway, just an auxiliary tool to converge to solution, it is reported as an efficient choice for the interaction.

It is important to make a distinction between solving the steady and unsteady flow problem. In literature, no results have been published for the application of the quasi-simultaneous

method to unsteady flow whereas for steady flow, extensive studies have been published e.g. Coenen [2], Bijleveld [13].

In the next section, the unsteady form of the quasi-simultaneous method is introduced.

4-2 Unsteady quasi-simultaneous method

It has been noted that interaction methods, except the simultaneous method, have been implemented mostly for the solution of steady flow. The derivations, theories and the approaches to explain the interaction boundary layer flows are based on steady flows. That reason behind this is as follows: the coupling techniques are developed to avoid solving the full Navier-Stokes equations. The splitting idea was initiated to keep the solution procedure as simple as possible. However, when the unsteady effects of the flow are also considered, the system becomes complicated: coupling the models in the two regions as well as the unsteady nature of the boundary layer constitute a complex problem. Hence, when unsteady effects are considered, it has been chosen either to solve the system simultaneously or using the the discretized Navier-Stokes equations coupled to an appropriate turbulence model.

The unsteady effects change the whole embodiment behind the coupling schemes. This can be explained considering Figure 4-3 where a "matched" solution is plotted. Here, it is assumed that the solutions of the viscous and the inviscid flow models will be the same when the system is converged. The main assumption behind this is that there *is* a "matched/converged" solution which, corresponds to the steady solution when time $t \rightarrow \infty$. However, for the unsteady boundary layer, there might not be a matched solution. The unsteady behaviour of the boundary layer is another research topic and a quite controversial area. Therefore, methods such as the Triple-Deck theory and the functional approach do not provide a precise explanation about the coupling procedure; they only serve as an auxiliary explanation for the unsteady case.

Keeping these primary differences in mind, the unsteady coupling techniques are investigated and a scheme for the quasi-simultaneous method is derived keeping the focus only on the direct and simultaneous method, because the quasi-simultaneous method can be viewed as a combination of these two.

Unsteady Direct Method

The unsteady process can be seen as the steady processes stopped at a certain time level. While the procedure stays same, only the embodiment behind it differs. This procedure can be seen schematically from Figure 4-6.

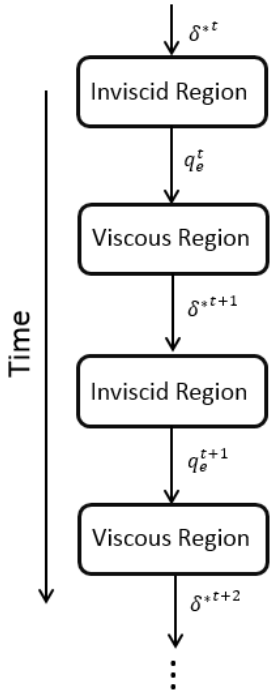

Figure 4-6: *Schematic explanation of the unsteady direct methods.*

The inviscid flow model calculates the velocity for a given displacement thickness; then, this displacement thickness is passed into the viscous region and by integrating the viscous model equations in time, the displacement thickness at the next time level is calculated which is the input for the edge velocity at that time level. The mathematical formulation can be described as:

$$\begin{cases} \boldsymbol{q_e}^t = P\left(\delta^{*^t}\right), \\ \delta^{*^{t+1}} = B^{-1}\left(\boldsymbol{q}_e^t\right), \end{cases} \tag{4-15}$$

where t denotes time iteration.

Unlike the steady method, this method will not cause the Goldstein singularity unless $t \to \infty$.

Simultaneous method

The simultaneous method implies that both the inviscid flow and the boundary layer equations are integrated in time to calculate the edge velocity and displacement thickness in the next time level. This procedure can be seen schematically from Figure 4-7.

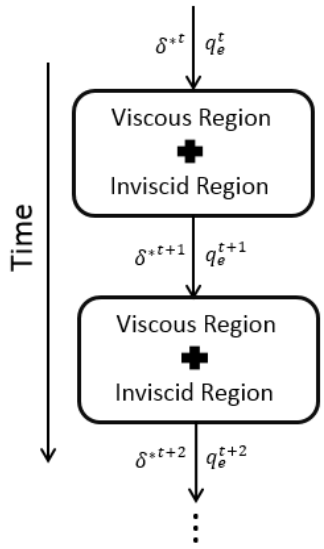

Figure 4-7: *Schematic explanation of the unsteady simultaneous method.*

The mathematical formulation is given as:

$$\begin{cases} \boldsymbol{q}_e^{t+1} = P\left(\delta^{*^t}\right), \\ \boldsymbol{q}_e^{t+1} = B\left(\delta^{*^t}\right). \end{cases} \tag{4-16}$$

The solution obtained with the simultaneous method corresponds to the solution of a non-linear system of equation which is integrated in time having the displacement thickness as an initial and edge velocity as a boundary condition to determine the both $\delta^{*^{t+1}}$ and q_e^{t+1} at the next time level (e.g. the Runge-Kutta scheme).

Unsteady Quasi-Simultaneous method

Having defined the unsteady direct and simultaneous methods, the quasi-simultaneous method which is derived basically by combining the advantages of these two method can be explained. It differs from the steady formulation since no matched solution is considered during the scheme. The procedure marches in time starting like the direct method: it integrates the edge velocity from previous time to next time level using the the displacement thickness at new time level and the boundary conditions on the corresponding time level as the input. However, when this edge velocity arrives in the boundary layer formulation, the direct method is put aside and a combination of $\boldsymbol{q_e}$ and δ^* is prescribed as a boundary condition, which is also called the interaction law, to the integral boundary layer equations (IBL). These two equations, the interaction law and the IBL equations, are solved simultaneously resulting in the displacement thickness *correction*, denoted by $\Delta\delta^*$ which is added to the displacement thickness at the previous time to calculate the one in the next time step. In order to clarify the procedure, consider Figure 4-8.

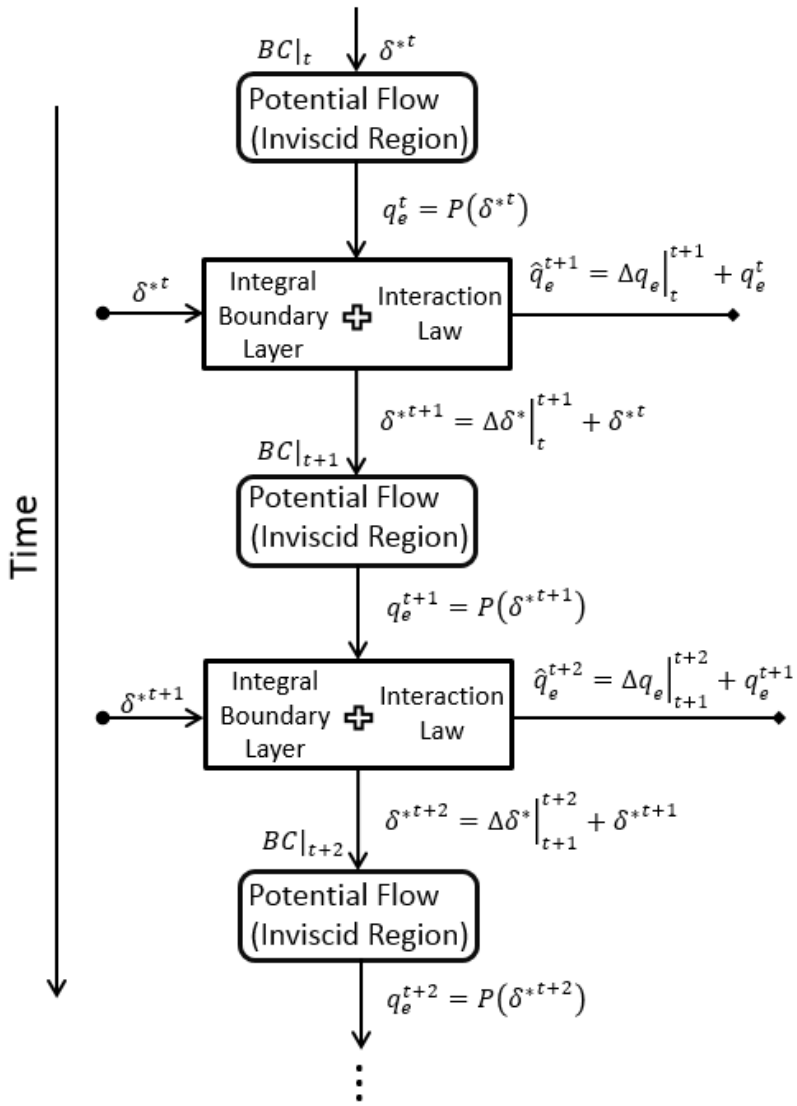

Figure 4-8: *Schematic explanation of the unsteady quasi-simultaneous method.*

Here the procedure resembles the direct method starting with updating the velocity using panel method:

$$\boldsymbol{q}_{e_P}^t = P\left(\delta^{*^t}\right).$$

Then, the simultaneous method is implemented to calculate the displacement thickness at next time level:

$$\begin{cases} \boldsymbol{q}_e^{t+1} = P\left(\delta^{*^t}\right), \\ \boldsymbol{q}_e^{t+1} = B\left(\delta^{*^t}\right). \end{cases}$$

However, here unlike in the simultaneous method, the interaction law I is used instead of the whole inviscid flow operator which yields the following form:

$$(I - B)\delta^{*^t} = 0. \tag{4-17}$$

Equation (4-17) results in a coupled non-linear system. After the time integration, it provides the displacement and the velocity at the new time level expressed in following equations:

$$\hat{\boldsymbol{q}}_{e_B}^{t+1} = \Delta \boldsymbol{q}_e|_t^{t+1} + \boldsymbol{q}_{e_P}^t, \tag{4-18a}$$
$$\delta^{*^{t+1}} = \Delta \delta^*|_t^{t+1} + \delta^{*^t}. \tag{4-18b}$$

It is important to emphasize that the solution of (4-17) provides only the corrections denoted by $\Delta \boldsymbol{q}_e|_t^{t+1}$ and $\Delta \delta^*|_t^{t+1}$ arisen from the viscous effects. Note that these *corrections* correspond to interaction terms $I(\delta^*)$. Cebeci *et al* [11] explained this relation as a sum of the inviscid velocity and a small perturbation arising from the presence of the boundary layer. This is caused by the fact that instead of the inviscid solver, the interaction law is employed (which is also the reason that why it is called *quasi*-simultaneous method). The role of the interaction law is to introduce the displacement of the boundary layer due to the viscous effects. In the same way the singularity arising form the inverse of the IBL operator is avoided for the steady coupling. Furthermore, notice that there is a hat $\hat{\boldsymbol{q}}_{e_B}$ in (4-18a) indicating that this velocity is not the real velocity at new time step. The reason behind that is the core difference between the steady and unsteady formulation of the quasi-simultaneous method.

Remember that the steady formulation of the quasi-simultaneous method has the following form:

$$\boldsymbol{q}_{e_B}^n - I(\delta^{*^n}) = \boldsymbol{q}_{e_P}^{n-1} - I(\delta^{*^{n-1}}). \tag{4-19}$$

In this formulation, it is known that for a converged, steady solution, the interaction terms will cancel out and the two edge velocities will be equal $\boldsymbol{q}_{e_B}^t = \boldsymbol{q}_{e_E}^{t-1}$. However, in the unsteady case, the aim is not to find a steady solution. Furthermore, there might be no steady solution.

In the unsteady formulation (4-18a), the interaction law has a direct effect on the velocity at the new time level. Taking into account that the interaction law is an approximation of the inviscid flow model, the new velocity computed by the quasi-simultaneous solution between the integral boundary layer equations and the interaction law, denoted by hat $\hat{\boldsymbol{q}}$, will not correspond to the real velocity at the new time level due to the fact that the simplifications introduced to obtain the interaction law inevitably cause loss of accuracy (Notice that this is

not the case in the steady case since the interaction law is an auxiliary tool only to improve the convergence rate). Therefore, the velocity given in (4-18a) is not considered, instead the displacement thickness (4-18b) is considered as an input to the inviscid solver with the corresponding time level's boundary conditions to find the velocity at the next time level. In this way, the information that had to be sacrificed to derive the interaction law, i.e. to avoid fully simultaneous solution, is aimed to be compensated partly by the inviscid flow model.

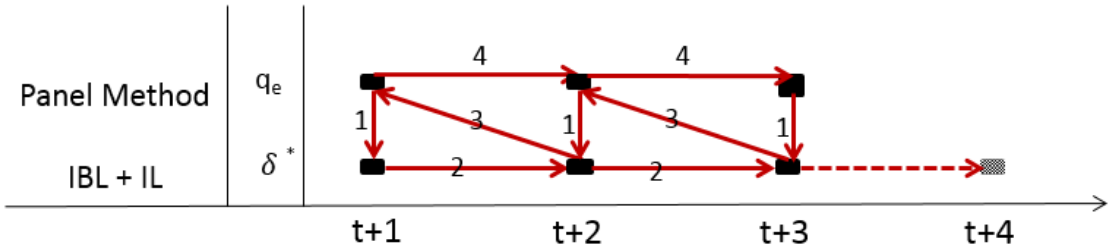

Figure 4-9: *Solution algorithm of the unsteady quasi-simultaneous method.*

This procedure is summarized in Figure 4-9.

The final form of the unsteady quasi-simultaneous method is given as:

$$\begin{cases} \hat{\boldsymbol{q}}_e^{t+1} - I\left(\delta^{*^t}\right) & = \boldsymbol{q}_e^t, \\ \hat{\boldsymbol{q}}_e^{t+1} - B\left(\delta^{*^t}\right) & = 0. \end{cases} \tag{4-20}$$

$$\left\{\boldsymbol{q}_e^{t+1} - P\left(\delta^{*^{t+1}}\right) \quad = 0, \right. \tag{4-21}$$

where $I[\delta^{*^t}] = \Delta \boldsymbol{q}_e|_t^{t+1}$ called interaction term and (4-18a) is the interaction law.

Unlike the steady case, in the unsteady quasi-simultaneous method, the interaction law does not vanish which makes it of a great importance not only for the convergence rate but also for the accuracy of the solution since it models the viscosity effect on the general problem. Therefore, the derivation of the interaction law becomes a significant issue in the unsteady case. As a rule of thump, an interaction term should carry as much physical information as possible in a form that is as simple as possible.

The derivation of the interaction law and the treatment of the coupled system caused by the quasi-simultaneous solution of the integral boundary layer equations and interaction law is explained in the next chapter.

4-3 Discussion about unsteady singularities

It has been mentioned that the Goldstein singularity is derived for the steady boundary layer when $t \to \infty$. However, when the unsteady case is considered, the nature of the boundary layer changes and brings about new physical phenomena. A comprehensive discussion of the

singularities in an unsteady boundary layer is published in reference [41] edited by Cebeci. This discussion contains seven articles written by pioneer names in the boundary layer theory and this section is based on these articles.

Cebeci [50] asserted that the singularities observed in a boundary layer can be divided into two classes. The first one includes the well-known Goldstein singularity. The criteria for this kind of singularity to occur are derived firstly by Moore, Rott, and Sears (known as MRS criteria) in 1955. They stated that to observe this type of singularity, the shear stress should vanish and the fluid should be at rest, i.e. $u = \partial u/\partial y = 0$. In this case, this corresponds particularly to the point where the skin friction, the wall shear stress, vanishes. This singularity is showed to be stemmed from the viscous character of the flow.

The second class of singularities is associated with the inviscid character of the flow. Moore, Rott, and Sears had seen this and pointed out that "in unsteady flow, the zero wall shear does not in general signify separation in the sense that the boundary layer leaves the wall." However, the reason and a rigorous proof of the existence of this second type of singularity had been a controversial topic for a long time. While Van Dommelen and Shen [20] and Dwyer and Sherman [51] have found supportive arguments for the existence of an unsteady singularity in their studies, Cebeci [44] denied its existence. Although Cebeci also encountered an evidence for the existence of this kind of singularity in one of his numerical experiment, he claimed that it is stemmed from the numerical method itself and the solution is smooth there: "a singularity cannot develop... at a finite time if the solution is free from singularities at earlier times". He meant the solution remains smooth for all finite time. However, this has been proved to be wrong. Van Dommelen and Shen [20] were the first ones who had come with a strong evidence and showed that there is a finite-time singularity caused by the intersection of two fluid particles at the same time which contradicts Cebeci's hypothesis. They showed that, unlike the Goldstein singularity, this new type of singularity has an inviscid character caused by the fact that the special set of equations obtained for the thickness of $O(\mathrm{Re}^{-1/2})$, see Figure 4-2, can no longer describe the flow because the amount of the separating layer marching into the inviscid flow becomes large compared to the middle inviscid layer thickness [45]. It has been shown by several researches independently that this new singularity reveals itself by blowing up of the boundary layer thickness while the wall shear remains non-zero. Van Dommelen and Shen were able to satisfy the conditions stated by Moore, Rott, and Sears for this type of singularity as well in their numerical experiment conducted on a boundary layer of a cylinder started impulsively. In other words, they found a point in the boundary layer, not on the wall, where the shear stress is zero and the fluid is stationary. This inviscid character singularity commonly known as "Van Dommelen singularity".

For more detailed information the reader should refer to the aforementioned literature, for only an insight to the unsteady boundary layer singularities is given here.

Chapter 5

Quasi-simultaneous solution

In the previous chapter, the unsteady quasi-simultaneous method is explained and it has been brought forward that in this algorithm the integral boundary layer equations and the interaction law are solved simultaneously. This chapters explains this quasi-simultaneous solution in detail and derives the resulting coupled system.

The integral boundary layer equations are given in the first chapter in a conservative integral form. Therefore, first, the conservative formulations of the integral boundary layer equations in integral and differential form are discussed. Furthermore, it is shown by Cousteix and Houdeville [52] and Bijleveld [13] that the integral boundary layer equations, both separately and coupled to the model for the inviscid flow region form an unconditionally hyperbolic system of partial differential equations. Toro [53] is used as the main reference for the theory on hyperbolic systems because it particularly approaches the subject from the fluid mechanics perspective. For the generalized eigenvalue problem, Datta [54] provides a good reference. More background and theory can be found in different textbooks such as [55, 56].

5-1 Hyperbolic partial differential equations

Mathematical models can very often be formulated either in differential or integral form. Furthermore, the equations can be formulated in different sets of primary variables. The common choice is the conserved variables since they entail computational advantages when the models take the form of conservations laws such as mass, momentum, energy *etc.*, that are conserved considering the conservation of mass, Newton's second law, and the law of conservation of energy, respectively. A large number of numerical methods have been developed based on this approach which are called the conservative methods.

As Seubers [28] followed an integral approach in the derivation of the governing equations of the viscous flow, the coupled system is also constructed in the integral form. Therefore, the following integral form is introduced:

$$\frac{\partial}{\partial t}\int_{\mathcal{V}} \boldsymbol{u}\mathrm{d}\mathcal{V} + \oint_{\partial\mathcal{V}} \boldsymbol{f}(\boldsymbol{u})\cdot\boldsymbol{n}\mathrm{d}\Gamma = 0, \tag{5-1}$$

where $\mathcal{V}$ is the control volume, $\boldsymbol{u}$ is the vector of conserved variables, and $\boldsymbol{f}(\boldsymbol{u})$ corresponds to the vector of fluxes. Assuming that the flow variables are sufficiently smooth, (5-1) can also be written in the differential form given as

$$\frac{\partial \boldsymbol{u}}{\partial t} + \mathrm{div}\boldsymbol{f}(\boldsymbol{u}) = 0. \tag{5-2}$$

Any set of partial differential equations which can be written in the above form (5-2) is called a system of conservation laws.

The vector of fluxes $\boldsymbol{f}(\boldsymbol{u})$ can be expanded as

$$\frac{\partial \boldsymbol{f}(\boldsymbol{u})}{\partial x} = \frac{\partial \boldsymbol{f}}{\partial \boldsymbol{u}}\frac{\partial \boldsymbol{u}}{\partial x}, \tag{5-3}$$

where $\partial\boldsymbol{f}/\partial\boldsymbol{u}$ is the Jacobian matrix corresponding to x given by

$$A_{ij} = \frac{\partial f_i(\boldsymbol{u})}{\partial u_j}. \tag{5-4}$$

Hence, (5-2) can be formulated in so-called the quasi-linear form:

$$\frac{\partial \boldsymbol{u}}{\partial t} + A(\boldsymbol{u})\frac{\partial \boldsymbol{u}}{\partial x} = 0. \tag{5-5}$$

In the above form (5-5), only the flux Jacobian corresponding to the x is considered. Taking into account the flux Jacobian corresponding to the t in order to discuss the most general case, (5-5) extends to

$$A^t(\boldsymbol{u})\frac{\partial \boldsymbol{u}}{\partial t} + A^x(\boldsymbol{u})\frac{\partial \boldsymbol{u}}{\partial x} = 0. \tag{5-6}$$

Equation 5-6 constitutes a generalized eigenvalue problem which can be written in following form:

$$A^x\boldsymbol{v} = \lambda A^t\boldsymbol{v}, \tag{5-7}$$

where $\boldsymbol{v}$ is the generalized eigenvector of A^x and A^t matrices and λ is the corresponding generalized eigenvector of A^x and A^t which, physically corresponds to the speed of propagation of the information. The eigenvalues λ_i of this system are the solutions of the characteristic polynomial:

$$|A^x - \lambda A^t| = \det(A^x - \lambda A^t) = 0. \tag{5-8}$$

If A^t matrix is invertible, (5-7) reduces to the standard eigenvalue problem with $A = \left[A^t\right]^{-1}\left[A^x\right]$ and the characteristic polynomial can be expressed as:

$$p(\lambda) = -\lambda^3 + \mathrm{Tr(A)}\lambda^2 - \mathrm{h(A)}\lambda + \det(\mathrm{A}). \tag{5-9}$$

The coefficients in (5-9) are defined as:

$$\mathrm{Tr(A)} = \lambda_1 + \lambda_2 + \lambda_3, \tag{5-10a}$$
$$\mathrm{h(A)} = \lambda_1\lambda_2 + \lambda_2\lambda_3 + \lambda_3\lambda_1, \tag{5-10b}$$
$$\det(\mathrm{A}) = \lambda_1\lambda_2\lambda_3, \tag{5-10c}$$

where $\lambda_1, \lambda_2, \lambda_3$ are the roots of (5-9) which correspond to the eigenvalues of the system.

A system (5-6) is said to be *hyperbolic* at a point (x, t) if A has m *real* eigenvalues $\lambda_1, ..., \lambda_m$ and a corresponding set of m linearly independent right eigenvectors $K^{(1)}, ..., K^{(m)}$. The system is said to be *strictly hyperbolic* if the eigenvalues λ_i are all distinct.

5-2 Coupled system

The integral boundary layer equations (2-10) are solved simultaneously with the interaction law which constitutes a coupled system of hyperbolic partial differential equations. The form of the interaction law (IL) is given in (4-18a). In this section, the appropriate interaction law is derived based on the detailed discussion of the inviscid flow model presented in Chapter 3.

Interaction law

It has been noted in Chapter 4 that the unsteady quasi-simultaneous scheme takes into account only the viscous effects during the quasi-simultaneous solution of the integral boundary layer equations and the interaction law, which is also the reason that the results are called the *corrections* as explained in Section 4.2. In order to calculate these corrections, the equation which gives the doublet distribution in the potential flow given in (3-37), is discretized by panel method given in fully matrix form as follows:

$$A\left(\boldsymbol{\mu_{inv}} + \boldsymbol{\mu_{vis}}\right) + B\left(\boldsymbol{\sigma_{inv}} + \boldsymbol{\sigma_{vis}}\right) = 0, \tag{5-11}$$

where A and B are $(N_b+N_w)\times(N_b+N_w)$ aerodynamic influence matrices. When the viscous and inviscid effects are considered individually, (5-11) becomes:

$$A\boldsymbol{\mu_{inv}} + B\boldsymbol{\sigma_{inv}} = 0, \tag{5-12a}$$
$$A\boldsymbol{\mu_{vis}} + B\boldsymbol{\sigma_{vis}} = 0. \tag{5-12b}$$

Recall the viscous source strength is given by (3-51):

$$\boldsymbol{\sigma_{vis}} \equiv \boldsymbol{v_n} = \frac{\partial}{\partial x}(\boldsymbol{q_e}\boldsymbol{\delta^*}).$$

Using (3-51) in (3-37b) and implementing the panel method (5-12b), an expression for μ_{vis} in terms of σ_{vis} can be found and as σ_{vis} is expressed in terms of the displacement thickness δ^*, the final expression for μ_{vis} can be formulated in terms of δ^*. An additional simplification is made: the influence of the wake region is neglected. This will affect the solution for lifting bodies as will be discussed in the last chapter. Finally, the following form is obtained regarding the viscous contributions:

$$A\boldsymbol{\mu_{vis}} + B\left(\frac{\partial}{\partial x}(\boldsymbol{q_e}\boldsymbol{\delta^*})\right) = 0. \tag{5-13}$$

Equation (5-13) can be solved for μ_{vis}

$$\boldsymbol{\mu_{vis}} = -A^{-1}B\left(\frac{\partial}{\partial x}(\boldsymbol{q_e}\boldsymbol{\delta^*})\right). \tag{5-14}$$

Then, using (3-37c), the velocity perturbation, i.e. *the interaction term*, can be calculated:

$$I[\delta^*]_m \equiv \Delta q_{e_m} = \left(\frac{\partial}{\partial x}(q_e\delta^*)\right)_m \boldsymbol{n} - \nabla_s \mu_{vis_m}, \tag{5-15}$$

where the operator ∇_s denotes the surface gradient.

Apart from neglecting the wake region, (5-15) is the general solution resulting from the viscous contributions solved numerically by means of the panel method. The calculated velocity perturbation is visualized in Figure 4-8.

Having defined the interaction term, the new velocity is calculated using the following *interaction law*:

$$\hat{\boldsymbol{q}}_e^{t+1} - I\left(\delta^*|_t^{t+1}\right) = \boldsymbol{q}_e^t. \tag{5-16}$$

Equation (5-16) expresses the relation between the simultaneous solution (IBL + IL) and the direct solution (inviscid flow model). The interaction term $I\left(\delta^*|_t^{t+1}\right)$ is found by (5-15) and it represents the effect of the viscosity on the inviscid flow acting on the boundary layer. Then, the interaction law is written as (for the ease of notation the hat is dropped):

$$\boldsymbol{q}_e^{t+1} - \sigma_{vis}^t \boldsymbol{n} + \nabla_s \mu_{vis}^t = \underbrace{\boldsymbol{q}_e^t}_{\text{known}} . \tag{5-17}$$

Notice that in (5-17), the right-hand side is already known from the solution of the inviscid flow model and it can even be decomposed into its x and $z-$velocity components, namely $\tilde{\boldsymbol{q}_x}$ and $\tilde{\boldsymbol{q}_z}$,

$$\boldsymbol{q_e} = \underbrace{\underbrace{\boldsymbol{q_{e_x}}}_{\text{known}} - \nabla_s \mu_{vis}}_{\tilde{\boldsymbol{q}}_{\boldsymbol{e_x}}} + \underbrace{\underbrace{\boldsymbol{q_{e_z}}}_{\text{known}} + \left(\frac{\partial}{\partial x}\left(q_e \delta^*\right)\right)\boldsymbol{n}}_{\tilde{\boldsymbol{q}}_{e_z}} \tag{5-18}$$

Construction of the coupled system

In order to express the interaction law in the same set of variables with the integral boundary layer equations, the normalized magnitude of the edge velocity is expressed as:

$$q_e = \frac{1}{Q_\infty}\sqrt{\left(|\boldsymbol{q_{e_x}} - \nabla_s \mu_{vis}|\right)^2 + \left(|\boldsymbol{q_{e_z}} + \sigma_{vis}\boldsymbol{n}|\right)^2}. \tag{5-19}$$

Taking the square of both sides of (5-19):

$$q_e^2 = \frac{1}{Q_\infty^2}\left(\left(|\boldsymbol{q_{e_x}} - \nabla_s \mu_{vis}|\right)^2 + \left(|\boldsymbol{q_{e_z}} + \sigma_{vis}\boldsymbol{n}|\right)^2\right). \tag{5-20}$$

In order to simplify the notation, the absolute value signs and subscripts that denotes the mth panel are removed taking into account that each term above indicates the length of the corresponding vector, (5-20) can be reformulated as

$$q_e^2 = \frac{1}{Q_\infty^2}\left(q_{e_x}^2 + q_{e_z}^2 - 2q_{e_x}|\nabla_s \mu_{vis}| + 2q_{e_z}\sigma_{vis} + |\nabla_s \mu_{vis}|^2 + (\sigma_{vis})^2\right). \tag{5-21}$$

Neglecting the last two terms using the fact that $\Delta q_e \ll q_e$, (5-21) becomes:

$$q_e^2 + \frac{1}{Q_\infty^2}2q_{e_x}|\nabla_s \mu_{vis}| - \frac{1}{Q_\infty^2}2q_{e_z}\sigma_{vis} = \frac{1}{Q_\infty^2}\left(q_{e_x}^2 + q_{e_z}^2\right). \tag{5-22}$$

The doublet distribution μ_{vis} is given by (5-14). Considering only the local effects (for the justifications the reader should refer to last chapter), (5-14) will reduce to the following form, specified on each panel,

$$\mu_{vis_m} = -K\sigma_{vis_m}, \tag{5-23}$$

where K is the $m-$th diagonal of the multiplication of $[A]^{-1}[B]$ matrix after localization, i.e. taking only the diagonals, calculated during the panel method. Retaining the gradient will result in a second order partial differential system, in order to avoid this, the gradient of the doublet distribution is approximated using first order backward finite differencing, considering the system in one dimension:

$$|\nabla_s \mu_{vis}| \equiv \frac{d}{dx}\left(\mu_{vis}\right) = \frac{(K\sigma_{vis})_{i-1} - (K\sigma_{vis})_i}{\Delta x}, \tag{5-24}$$

where Δx is the distance between the two collocation points i and $i-1$ on the panels used by the discretization of the inviscid flow model. However, note that $(K\sigma_{vis})$ term has been projected on the panels in order to use finite differencing. Considering the the fact that the unknowns at panel $i-1$ have been already calculated, these terms can be shifted into the right-hand side,

$$q_e^2 - \sigma_{vis}(C_x + C_z) = \frac{1}{Q_\infty^2}\left(q_{e_x}^2 + q_{e_z}^2\right) - \frac{1}{Q_\infty^2} 2q_{e_x} \frac{(K\sigma_{vis})_{i-1}}{\Delta x}, \tag{5-25}$$

where

$$C_x = \frac{2q_{e_x}K}{Q_\infty^2 \Delta x},$$
$$C_z = \frac{2q_{e_z}}{Q_\infty^2}.$$

Taking the time-derivative of the both sides of (5-25) yields:

$$\frac{\partial q_e^2}{\partial t} - \frac{\partial}{\partial t}\left(\sigma_{vis}(C_x + C_z)\right) = \frac{\partial}{\partial t}\left(\frac{1}{Q_\infty^2}\left(q_{e_x}^2 + q_{e_z}^2\right) - \frac{1}{Q_\infty^2} 2q_{e_x} \frac{(K\sigma_{vis})_{i-1}}{\Delta x}\right). \tag{5-26}$$

Same approach followed in (5-26) is also followed in order to avoid mixed derivative in the second term of left-hand side in (5-26):

$$\frac{\partial}{\partial t}\left(\sigma_{vis}(C_x + C_z)\right) = \frac{(E\sigma_{vis})^t - (E\sigma_{vis})^{t-1}}{\Delta t}, \tag{5-27}$$

where $E^t := (C_x + C_z)^t$.

Again, shifting the terms corresponding to the previous time level into the right hand into right-hand side and using (3-51), (5-26) becomes:

$$\frac{\partial q_e^2}{\partial t} - F\frac{\partial}{\partial x}(q_e \delta^*) = \frac{\partial}{\partial t}\left(\frac{1}{Q_\infty^2}\left(q_{e_x}^2 + q_{e_z}^2\right)\right) - \frac{\partial}{\partial t}\left(\frac{1}{Q_\infty^2} 2q_{e_x} \frac{(K\sigma_{vis})_{i-1}}{\Delta x}\right) - \frac{(E\sigma_{vis})^{t-1}}{\Delta t}, \tag{5-28}$$

where $F = E^t/\Delta t$.

After non-dimensionalizing (5-28) the final form of the interaction law becomes:

$$\frac{\partial q_e^2}{\partial t} - Fc\frac{\partial}{\partial x}(q_e\delta^*) = \frac{\partial}{\partial t}\left(\frac{1}{Q_\infty^2}\left(q_{e_x}^2 + q_{e_z}^2\right)\right) - \frac{\partial}{\partial t}\left(\frac{1}{Q_\infty^2}2q_{e_x}\frac{(K\sigma_{vis})_{i-1}}{\Delta x}\right) - \frac{(E\sigma_{vis})^{t-1}}{\Delta t}\frac{L}{Q_\infty}. \quad (5\text{-}29)$$

Substituting (5-29) into (2-10), the final set of equations for the coupled system is obtained:

$$\frac{\partial}{\partial t}\int_{\mathcal{V}} \boldsymbol{f}^t(\boldsymbol{u})\mathrm{d}\mathcal{V} + \int_{\mathcal{V}} \boldsymbol{g}^t(\boldsymbol{u})\frac{\partial \boldsymbol{u}}{\partial t}\mathrm{d}\mathcal{V} + [\boldsymbol{f}^x(\boldsymbol{u})]_{\partial\mathcal{V}^-}^{\partial\mathcal{V}^+} + \int_{\mathcal{V}} \boldsymbol{g}^x(\boldsymbol{u})\frac{\partial \boldsymbol{u}}{\partial x}\mathrm{d}\mathcal{V} = \int_{\mathcal{V}} \boldsymbol{s}(\boldsymbol{u})\mathrm{d}\mathcal{V}$$

$$\boldsymbol{u} = \begin{bmatrix} \delta^*/c \\ \varepsilon/c \\ q_e \end{bmatrix}, \quad (5\text{-}30a)$$

$$\boldsymbol{f}^t(\boldsymbol{u}) = \begin{bmatrix} -q_e & 0 & 0 \\ 0 & -q_e^2 & 0 \\ 0 & 0 & q_e \end{bmatrix}\boldsymbol{u}, \quad (5\text{-}30b)$$

$$\boldsymbol{f}^x(\boldsymbol{u}) = \begin{bmatrix} q_e^2 & -q_e^2 & 0 \\ q_e^3 H_k & -q_e^3 H_k & 0 \\ 0 & 0 & 0 \end{bmatrix}\boldsymbol{u}, \quad (5\text{-}30c)$$

$$\boldsymbol{g}^t(\boldsymbol{u}) = \begin{bmatrix} 0 & 0 & 0 \\ 0 & 0 & 2q_e\varepsilon/c \\ 0 & 0 & 0 \end{bmatrix}, \quad (5\text{-}30d)$$

$$\boldsymbol{g}^x(\boldsymbol{u}) = \begin{bmatrix} 0 & 0 & -q_e\delta^*/c \\ 0 & 0 & 0 \\ -Fq_ec & 0 & -F\delta^* \end{bmatrix}, \quad (5\text{-}30e)$$

$$\boldsymbol{s}(\boldsymbol{u}) = \begin{bmatrix} \frac{1}{2c}C_f \\ \frac{2}{c}\mathrm{Re}_\delta^{-1}\mathcal{D}u_e^3 \\ \frac{\partial}{\partial t}\left(\frac{1}{Q_\infty^2}\left(q_{e_x}^2 + q_{e_z}^2\right) - \frac{1}{Q_\infty^2}2q_{e_x}\frac{(K\sigma_{vis})_{i-1}}{\Delta x}\right) - \frac{(E\sigma_{vis})^{t-1}}{\Delta t}\frac{L}{Q_\infty} \end{bmatrix}. \quad (5\text{-}30f)$$

As it can be seen from (5-30), the interaction introduced several non-conservative terms in the system of partial differential equations. Also, implementing the interaction law, it is now possible to substitute the derivative terms in the source term (2-10d) in non-conservative matrices $\boldsymbol{g}^t(\boldsymbol{u})$ and $\boldsymbol{g}^x(\boldsymbol{u})$.

The flux Jacobians are calculated using following expressions:

$$A^t_{ij}(\boldsymbol{u}) = \frac{\partial f^t_i(\boldsymbol{u})}{\partial u_j} + g^t_{ij}(\boldsymbol{u}),$$
$$A^x_{ij}(\boldsymbol{u}) = \frac{\partial f^x_i(\boldsymbol{u})}{\partial u_j} + g^x_{ij}(\boldsymbol{u}),$$

which yields

$$A^t_{ij}(\boldsymbol{u}) = \begin{bmatrix} -q_e & 0 & -\delta^*/c \\ 0 & -q_e^2 & 0 \\ 0 & 0 & 2q_e \end{bmatrix}, \tag{5-31a}$$

$$A^x_{ij}(\boldsymbol{u}) = \begin{bmatrix} q_e^2 & -q_e^2 & -\frac{q_e\delta^*(H+2)}{Hc} \\ q_e^3 H_k & -q_e^3 H_k & -\frac{3H_k q_e^2 \delta^*}{Hc} \\ -Fq_e c & 0 & -F\delta^* \end{bmatrix} + \frac{dH_k}{dH}\begin{bmatrix} 0 & 0 & 0 \\ -(H+1)q_e^3 & Hq_e^3 & 0 \\ 0 & 0 & 0 \end{bmatrix} + \frac{\partial H_k}{\partial q_e}\begin{bmatrix} 0 & 0 & 0 \\ 0 & 0 & -\frac{q_e^3\delta^*}{Hc} \\ 0 & 0 & 0 \end{bmatrix}. \tag{5-31b}$$

Characteristic polynomial

The characteristic polynomial (5-9) of the coupled system given in (5-30) is expressed in the following form:

$$p(\lambda) = -\lambda^3 + \mathrm{Tr(A)}\lambda^2 - \mathrm{h(A)}\lambda + \det(\mathrm{A})$$

where

$$\mathrm{Tr(A)} = -q_e\left(1 + H\left(\frac{dH_k}{dH} - \frac{H_k}{H}\right)\right), \tag{5-32a}$$
$$\mathrm{h(A)} = q_e^2\frac{dH_k}{dH} - L\left(1 + \frac{1}{H}\right), \tag{5-32b}$$
$$\det(\mathrm{A}) = \frac{Lq_e}{2}\left(H_k\left(\frac{1}{H} - H\right) + \frac{dH_k}{dH}(H+1) + \frac{q_e}{H}\frac{\partial H_k}{\partial q_e}\right). \tag{5-32c}$$

A new non-dimensional parameter, the interaction law coefficient, has been defined in (5-32) as:

$$L := F\delta^* \tag{5-33}$$

and it represents the effect of the interaction law on the system.

Using Vieta's substitution, the discriminant of (5-9) can be calculated as:

$$Q = \frac{3\mathrm{h}(A) - \mathrm{Tr}(A)^2}{9}, \tag{5-34a}$$

$$R = \frac{-9\mathrm{Tr}(A)\mathrm{h}(A) + 27\det(A) + 2\mathrm{Tr}(A)^3}{54}, \tag{5-34b}$$

$$\Delta_s = Q^3 + R^2. \tag{5-34c}$$

The discriminant of the system provides information about the eigenvalues which can be used to conclude if the system is *(strictly) hyperbolic* using the definition given in end of the previous section. If the polynomial discriminant $\Delta_s > 0$, one root is real and two are complex conjugates, then the system is *not hyperbolic*; if $\Delta_s = 0$, all roots are real and at least two are equal, then the system is *hyperbolic*; and if $\Delta_s < 0$, all roots are real and unequal, then is system is *strictly hyperbolic*.

Chapter 6

Results

The unsteady quasi-simultaneous scheme is introduced in Chapter 4. As a part of this scheme, the integral boundary layer equations are solved with the interaction law as the boundary condition and the resulting coupled system is derived in Chapter 5. Furthermore, the necessary conditions for a partial differential equation to be hyperbolic have been explained in the same chapter. In this chapter, the effect of the interaction law on the solution of the coupled system is explained.

First, appropriate closure relations have to be chosen to complement the integral boundary layer equation. Laminar flow is considered and the following closure relations for the shape factor and the skin friction are used [12]:

$$H_k(H) = \begin{cases} 1.528 + 0.0111\frac{(H-4.35)^2}{H+1} - 0.0278\frac{(H-4.35)^3}{H+1} \\ \qquad -0.0002[(H-4.35)H]^2 & H < 4.35, \\ 1.528 + 0.015\frac{(H-4.35)^2}{H} & H > 4.35 \end{cases} \tag{6-1}$$

$$C_f(H) = \begin{cases} \frac{1}{2}\left(-0.07 + 0.0727\frac{(5-5-H)^3}{H+1}\right) & H < 5.5, \\ \frac{1}{2}\left(-0.07 + 0.015\left(1 - \frac{1}{H-4.5}\right)^2\right) & H > 5.5 \end{cases} \tag{6-2}$$

Because of the difficulties in interpreting the eigenvalues of the system (5-30), the discriminant of the characteristic polynomial (5-9) is calculated by means of Vieta's substitution (5-34).

Figure 6-1 shows the discriminant of the system when the interaction law coefficient (5-33) is set to zero for the different values of the shape factor.

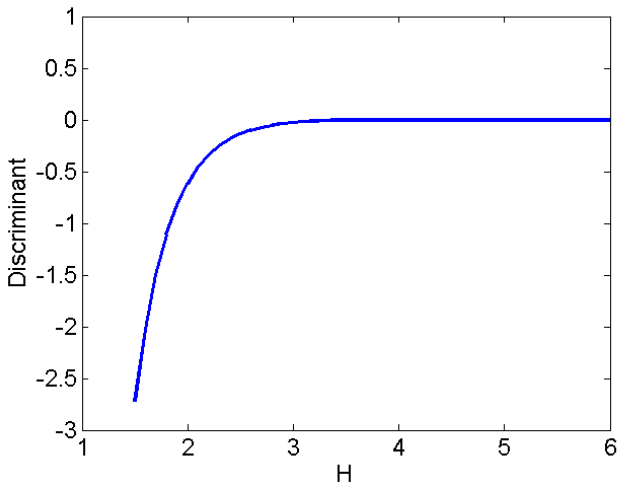

Figure 6-1: *The changes in the discriminant of the characteristic polynomial when the interaction law coefficient is set to zero.*

Figure 6-1 shows that the discriminant of the characteristic polynomial of A matrix approaches to zero as the shape factor increases. This means that two eigenvalues of the system become identical beyond a certain value of H (the sum can be seen in (5-32b)) and the other eigenvalue is calculated as zero. In the discussion about the unsteady singularities in the boundary layers, it has been noted that the singularity behaviour is associated with the shear stress by Moore, Rott, and Sears. Their reasoning was in order to observe a singularity in a boundary layer (steady or unsteady), the shear stress should vanish and the fluid should be at rest. Therefore, the skin friction coefficient, which indicates the shear stress at the *wall*, is plotted in Figure 6-2 in order to see if the value where the discriminant vanishes corresponds to the value at which the wall shear stress vanishes.

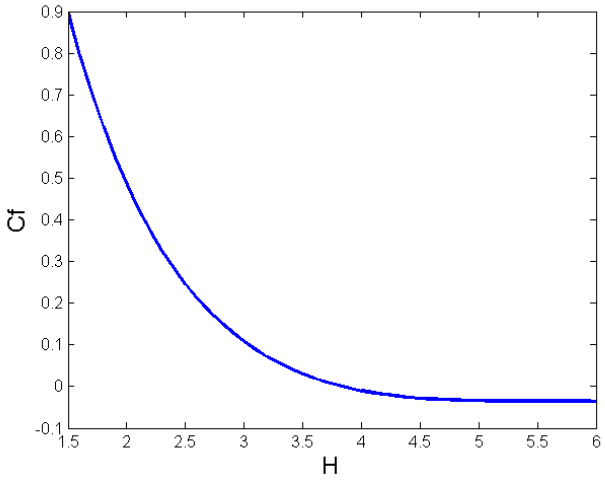

Figure 6-2: *Behaviour of the skin friction according to shape factor.*

Both Figures 6-1 and 6-2 show a similar trend. Both curves have an interval between $3.9 \leq H \leq 4.2$ where the skin friction and the discriminant approach to zero. This would suggest the presence of a Goldstein-type viscous character singularity. In order to check if the matrix is defective there, the eigenvectors are computed and three different eigenvectors are found which implies that the geometric multiplicity is *not* less then its algebraic multiplicity and consequently the matrix is not defective. This agrees with the discussion of the singularity behaviour in unsteady flows in Section 4.3. It has been noted that in unsteady flow, there is no Goldstein-type (viscous character) singularity present. On the other hand, this behaviour might correspond to a Van Dommelen singularity since it has been noted in [45] that Shen and Nenni also observed a singularity that comes about as an intersection of characteristics. However, Van Dommelen and Shen explained the primary physics, though it is still a controversial topic, behind this type of unsteady singularity as "...it turned out that the solution becomes singular because part of the vorticity layer moves away from the wall in an inviscid manner, while essentially preserving its diffusion-determined thickness". Since the coupled system is not able to include this physics and the lack of theoretical consensus, and a general criterum, it is not possible to conclude a Van Dommelen type singularity is present solely based on the results displayed in Figures 6-1 and 6-2, and the characteristics.

After seeing the behaviour of the system without the interaction, next the effect of the interaction law on the behaviour of the system is investigated. The coupled system (5-30) shows a new term in its flux Jacobian A^x_{ij} (5-32a):

$$\frac{\partial H_k}{\partial q_e}. \tag{6-3}$$

This term governs the effect of the interaction law on the integral boundary layer closure. Seubers [28] also encountered similar terms e.g. $\partial H_k/\partial \delta^*$ and $\partial H_k/\partial \varepsilon$. However, he was able to relate these terms to $\underline{\mathrm{H}}_k/\underline{\mathrm{H}}$ by means of the closure relations, so that he can evaluate them expressed as the second matrix in (5-32a). However, this is not the case when it comes to (6-3) since there is no closure relation derived as it is done for the integral boundary layer quantities. In order to fill this gap, a numerical experiment is conducted using a design code (XFOIL) developed by Drela [10, 57].

A simple, symmetric airfoil (NACA 0012) is chosen and for a slight change in q_e, the changes in H_k are plotted along the chord for $Re = 3.10^5$ in Figure 6-3.

Figure 6-3a shows that there is a sudden jump at around chord length of 0.9, this point corresponds to the laminar-turbulent transition point, i.e. where the laminar flow starts to be turbulent. The behaviour of the derivative of H_k (6-3) can be interpreted before transition which is plotted in Figure 6-3b. It is observed that magnitude of the derivative of H_k (6-3) never exceeds 0.5 which is at most order unity. Similar trends have been observed for other airfoils in the laminar flow, i.e. before the transition point. Therefore, the numerical experiment for (6-3) provides a reasonable approximation for laminar flow.

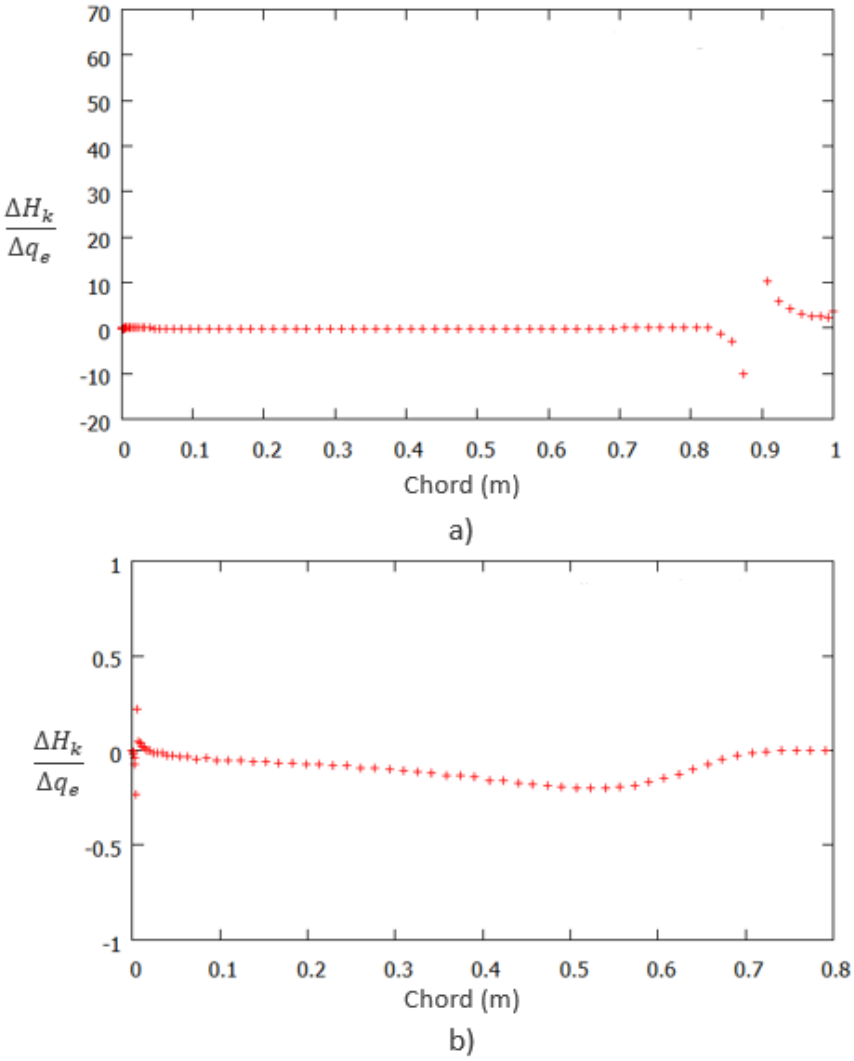

Figure 6-3: *The numerical experiment conducted on airfoil NACA 0012 in order to interpret* (6-3)*: a) Full chord length and the behaviour of* (6-3)*, b) Focused on the laminar region.*

Having an approximation for the new term (6-3), the effect of the interaction law coefficient (5-33) is investigated.

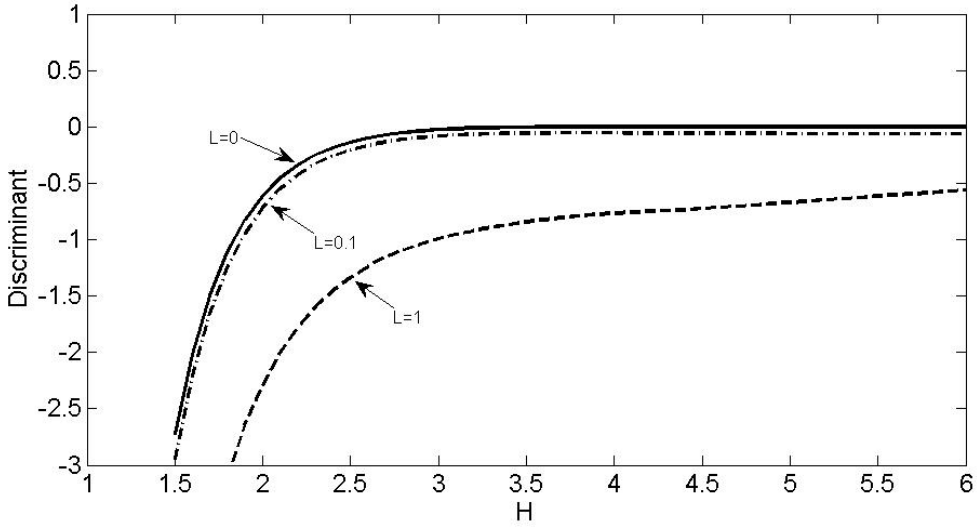

Figure 6-4: *The effect of the interaction law coefficient on the coupled system.*

Figure 6-4 show that including the interaction law, the discriminant of the characteristic polynomial shifts towards negative values which means that the two same eigenvalues become distinct with another nonzero distinct eigenvalue. Hence, the system becomes strictly hyperbolic and a possible Van Dommelen Singularity is avoided.

Recall that the interaction law coefficient is defined in (5-33) as:

$$L := \frac{(C_z + C_x)\,\delta^*}{\Delta t}.$$

The only term changes in this formulation is the time step Δt (note that the Δx term in C_x is the distance between the collocation points in panels prescribed in the inviscid flow model). It can be deduced from this definition that decreasing the time-step size will cause an increase in the interaction law coefficient and the effect of an increase in the interaction law coefficient is illustrated in Figure 6-4. Hence, an optimum step size can be find numerically which makes the system strictly hyperbolic.

Chapter 7

Conclusions and Discussions

In this thesis, the viscous-inviscid interaction schemes are investigated to be employed for the prediction of the aerodynamical characteristics of unsteady, incompressible flow around the wind turbine blade sections. The investigation is focused on the quasi-simultaneous scheme since it has been shown to be a rapidly convergent scheme in the case of steady flow. The differences between the idea behind the steady and unsteady viscous-inviscid interaction schemes are pointed out. A new scheme of the quasi-simultaneous scheme is introduced to solve the unsteady flow, using an interaction law specifically designed for the coupling of the unsteady models. The coupled system which is a resultant of the quasi-simultaneous solution is constructed. The effect of the interaction law on the system is investigated. The possible singularities that can occur are explained.

Discussion

It has been noted that during the derivations, some simplifications have been made that could negatively influence the accuracy of the solutions. Here these simplifications are discussed.

The discussion starts with the derivation of the panel based interaction law, specifically the derivation of the doublet strength (5-14). Expressing the doublet strength in terms of the source strength, there is an inverse and multiplication operation of two matrices A and B. These matrices are called the aerodynamic influence matrices and have a physical meaning: They express the effect of the $n-$th panel on the $m-$th panel. In their current form they are dense matrices. And taking the inverse of a dense matrix is an expensive operation. The argument here is: If one uses the dense matrix operations to obtain the interaction law, would it be worthwhile to derive an interaction law at all? When solving the interaction problem quasi-simultaneously is as much computationally expensive as solving it simultaneously, why would one use the quasi-simultaneous method? This argument implies an essential need for further simplification.

Following the reasoning of the question above, a simplification approach is offered whereby only the diagonals of A and B matrices are kept that corresponds, physically, to limit the

effect of the $n-$th panel on itself. This approach implies that in every panel, only the local source and doublet distributions are considered and the attention is restricted only to the local viscous effects. Using this approach, A matrix becomes easily invertible and $[A]^{-1}[B]$ multiplication can be easily calculated. Hence, it is possible to express (5-15) as a simple relation between displacement thickness and edge velocity, $f(\delta^*) = Cq_e$ where C is some constant. Note that, the aerodynamic influence coefficients A_{mn} and B_{mn} are known. The physical information that is lost when the off-diagonals are ignored is aimed to be compensated when the new δ^* is passed into the inviscid solver. In other words, every panel is updated by including the local viscous effects, then a new displacement thickness is calculated. This displacement thickness is then passed into the inviscid flow model where the global effects are also included. Hence, the only information loss is due to the nonlocal effect of σ_{vis}.

It is important to note that in the approximation, the presence of the singularity on the wake is also neglected. This simplification becomes important especially for the doublet strength since the effect of the wake is felt along the whole body. Neglecting the wake region corresponds to neglecting the effect of the wake on the body, particularly on the lifting properties. This effect could have been considered by adding one additional panel along the wake and by Helmholtz theorem, namely the Kutta condition, the doublet strength on this panel could have been related to the doublet strength on the body which means the doublet strength on the wake is known when the doublet strength on the body is known. The corresponding source strength can be modelled by a one or two layers approximation which basically has the same form as for the body (3-51). Using this wake implementation, the number of collocation points will increase by one and A and B matrices become $(N+1) \times (N+1)$ matrices. The physical correspondence to the diagonals will stay valid but during the local-effect-simplification, certain information will be lost again. In other words, by neglecting non-diagonal terms, almost all the effects of the wake which had been introduced are lost. Therefore, the whole wake region is ignored in the formulation of the viscous contribution and its effects are left to the inviscid flow model. But, as explained earlier, this is inevitable since without any sacrifice, it is not possible to find an approximation that can be incorporated in an efficient VII scheme.

Another important issue is the occurrence of unsteady singularities. As discussed earlier there is not a commonly accepted theory on the nature and physical mechanisms underlying these kinds of singularities. It is noted by several authors that the occurrence of these singularities has been observed when two characteristics intersect which corresponds to the case occurred in this research. However, since, unlike Goldstein singularity, this subject is still controversial, it has been avoided to make bold claims without a simulation.

Resume

The implementation of the current scheme and the interaction law could not be realized because of the time issues. However, a new unsteady scheme is introduced and a new interaction law is derived which is shown to ensure that the coupled system is strictly hyperbolic by making the same eigenvalues distinct avoiding a possible unsteady singularity. The research will continue with the stability analysis of the coupled system then according to the results, the new interaction law will be implemented in two/three dimensional incompressible unsteady solver which is currently being developed by Seubers [28] and the results will be evaluated to

see if the new quasi-simultaneous scheme yields accurate results compared to the experiments and if any unsteady singularity occurs as expected.

Bibliography

[1] M. Drela, "Three dimensional integral boundary layer formulation for general configurations," in *21st AIAA Computational Fluid Dynamics Conference*, (San Diego, CA), 2013.

[2] E. G. M. Coenen, *Viscous-inviscid interaction with the quasi-simultaneous method for 2D and 3D aerodynamic flow.* PhD thesis, University of Groningen, The Netherlands, 2001.

[3] H. Ozdemir and B. H. Garrel van, A., "Development of a 2d unsteady viscous-inviscid interaction method for wind turbine applications," in *ICWE13*, (Amsterdam, the Netherlands), 2011.

[4] H. Ozdemir, "Numerical solution of 2d unsteady integral boundary layer equations with a discontinuous galerkin method," in *European Workshop on High Order Nonlinear Numerical Methods for Evolutionary PDEs: Theory and Applications*, (Trento, Italy), 2011.

[5] H. Ozdemir and E. Boogaard van, "Solving the integral boundary layer equations with a discontinuous galerkin method," in *EWEA-2011*, (Brussels, Belgium), 2011.

[6] H. Schlichting and K. Gersten, *Boundary Layer Theory.* Springer, 8th ed., 2000.

[7] J. Le Balleur, "Couplage visqueux-non visqueux: methode numerique et applications aux ecoulements bidimensionnels transsoniques et supersoniques," Tech. Rep. 2:65-67, Office National d'Etudes et de Recherches Aerospatiales, France, 1978.

[8] L. Wigton and M. Holt, "Viscous-inviscid interaction in transonic flow," tech. rep., University of Berkeley, 1987.

[9] R. Houwink and A. E. P. Veldman, "Steady and unsteady separated flow computation for transonic airfoils." AIAA paper 84–1618, 1984.

[10] M. Drela and M. Giles, "Viscous-inviscid analysis of transonic and low reynolds number airfoils," *AIAA Journal*, vol. 25, no. 10, pp. 1347–1355, 1987.

[11] T. Cebeci, R. Clark, K. Chang, and N. Halsey, "Airfoils with separation and the resulting wakes," *Journal of Fluid Mechanics*, vol. 163, pp. 323–347, 1986.

[12] B. A. Nishida, *Fully simultaneous coupling of the full potential equation and the integral boundary layer equations in three dimensions*. PhD thesis, Massachusetts Institute of Technology, USA, 1996.

[13] H. A. Bijleveld, *Application of Quasi-Simultaneous interaction method for the determination of the aerodynamic forces on wind turbine blades*. PhD thesis, University of Groningen, The Netherlands, 2013.

[14] T. Swafford, D. Huddelston, J. Busby, and B. L. Chesser, "Computation of steady and unsteady quasi-one-dimensional viscous/inviscid interacting internal flows at subsonic, transonic, and supersonic mach numbers," tech. rep., NSF Engineering research center for computational field simulation, 1992.

[15] T. Cebeci, M. Platzer, H. Jang, and H. Chen, "Inviscid-viscous interaction approach to the calculation of dynamic stall initiation on airfoils," *Journal of Turbomachinery*, vol. 115(4), pp. 714–723, 1993.

[16] L. Bermudez, A. Velazquez, and M. A., "Inviscid-viscous method for the simulation of the turbulent unsteady wind turbune airfoil flow," *Journal of Wind Engineering and Industrial Aerodynamics*, vol. 90, pp. 643–661, 2002.

[17] R. Garcia, *Unsteady Viscous-Inviscid Interaction Technique for Wind Turbine Airfoils*. PhD thesis, Denmark Technical University, Denmark, 2011.

[18] R. Lock and B. Williams, "Viscous-inviscid interactions in external aerodynamics," *Progress in Aerospace Sciences*, vol. 24, pp. 51–171, Jan. 1987.

[19] B. Williams, "Viscous-inviscid interaction schemes for external aerodynamics," tech. rep., Aerodynamics Department, Royal Aerospace Establishment, Farnborough, UK, 1991.

[20] L. Dommelen van and S. Shen, "The spontaneous generation of the singularity in a separating laminar boundary layer," *Journal of Computational Physics*, vol. 38, pp. 125–140, 1980.

[21] R. Henkes and A. Veldman, "On the breakdown of the steady and unsteady interacting boundary-layer description," *Journal of Fluid Mechanics*, vol. 179, pp. 513–529, 1987.

[22] K. Stewartson, "Multistructured boundary layers on flat plates and related bodies," *Archive of Applied Mechanics*, vol. 14, pp. 145–239, 1974.

[23] S. Goldstein, "Laminar boundary layer-flow near a position of separation," *Quarterly Journal of Mechanics and Applied Mathematics*, vol. 1, pp. 43–69, 1948.

[24] A. E. P. Veldman, "New, quasi-simultaneous method to calculate interacting boundary layers," *AIAA*, vol. 19, pp. 79–85, 1981.

[25] D. Catherall and K. W. Mangler, "The integration of the two-dimensional laminar boundary-layer equations past the point of vanishing skin friction," *Journal of Fluid Mechanics*, vol. 26, no. 01, 1966.

[26] A. E. P. Veldman, "A simple interaction law for viscous-inviscid interaction," *Journal of Engineering Mathematics*, vol. 65, pp. 367–383, Aug. 2009.

[27] A. E. P. Veldman, J. Lindhout, E. Boer de, and M. Somers, *Numerical and Physical Aspects of Aerodynamic Flow IV*, ch. Vistrafs: a simulation method for strongly-interacting viscous transonic flow, pp. 37–51. Berlin: Springer Verlag, 1990.

[28] H. Seubers, "Nonconservative discontinuous galerkin discretization applied to integral boundary layer equations (draft)," Master's thesis, Technical University of Delft, the Netherlands, 2013.

[29] B. Munson, D. Young, T. Okiishi, and W. Huebsch, *Fundamentals of Fluid Mechanics*. Jonh Wiley and Sons, 6th ed., 2009.

[30] F. White, *Viscous Fluid Flow*. New York: McGraw-Hill, Inc., 3rd ed., 2006.

[31] B. van Es, "Comparison and application of unsteady integral boundary layer methods using various numerical schemes," Master's thesis, Technical University of Delft, the Netherlands, 2009.

[32] J. Moran, *An introduction to Theoretical and Computational Aerodynamics*. John Wiley and Sons, 1984.

[33] J. Katz and A. Plotkin, *Low Speed Aerodynamics*. Singapore: McGraw-Hill, Inc., internatiol ed., 1991.

[34] A. Garrel van, "Development of a Wind Turbine Rotor Flow Panel Method," Tech. Rep. December, Energy Research Centre of the Netherlands, Petten, 2011.

[35] L. Erickson, "Panel Methods – An introduction," Tech. Rep. TP2995, NASA, 1990.

[36] M. Lighthill, "On displacement thickness," *Journal of Fluid Mechanics*, vol. 4, pp. 383–392, 1958.

[37] J. Le Balleur, "Viscid-inviscid coupling calculations for two-and three-dimensional flows," tech. rep., Von Karman Institute for fluid dynamics lecture series, March 29 – April 2 1982.

[38] R. Bartels, *An interacting boundary layer method for unsteady compressible flows*. PhD thesis, Iowa State University, USA, 1994.

[39] R. Bartels, "On an asymptotically consistent unsteady interacting boundary layer," Tech. Rep. TM-214868, Langley Research Center, Hampton, Virginia, 2007.

[40] A. Garrel van. personal communication.

[41] T. Cebeci, ed., *Numerical and Physical Aspects of Aerodynamic Flow*. Springer, 1982.

[42] A. Messitie, "Boundary layer flow near the trailing edge of a flat plate," *SIAM Journal of Applied Mathematics*, vol. 18, pp. 241–257, 1970.

[43] G. Brune, P. Rubbert, and N. T.C., "A new approach to inviscid flow/boundary layer matching," *AIAA*, vol. 74, no. 601, 1974.

[44] K. Wang, *Numerical and Physical Aspects of Aerodynamic Flow*, ch. On the current controversy about unsteady separation. In Cebeci [41], 1982.

[45] L. Dommelen van and S. Shen, *Numerical and Physical Aspects of Aerodynamic Flow*, ch. The genesis of separation. In Cebeci [41], 1982.

[46] J. Carter, "Viscous-inviscid interaction analysis of turbulent separated flow," *AIAA*, vol. 81, no. 1241, 1981.

[47] L. Lees and B. Reeves, "Supersonic separated and reattaching laminar flows: I. general theory and application to adiabatic boundary-layer shock-wave interactions," *AIAA*, vol. 2, no. 1907-1920, 1964.

[48] K. Stewartson and P. G. Williams, "Self-Induced Separation," *Proceedings of the Royal Society A: Mathematical, Physical and Engineering Sciences*, vol. 312, no. 1509, pp. 181–206, 1969.

[49] B. Williams and P. D. Smith, *Numerical and Physical Aspects of Aerodynamic Flow IV*, ch. Coupling procedures for viscous-inviscid interaction for attached and separated flows of swept and tapered wings, pp. 53–70. Berlin: Springer Verlag, 1990.

[50] T. Cebeci, *Numerical and Physical Aspects of Aerodynamic Flow*, ch. Unsteady separation. In [41], 1982.

[51] H. Dwyer and S. F.S., *Numerical and Physical Aspects of Aerodynamic Flow*, ch. Some characteristics of unsteady two- and three-dimensionl reversed boundary-layer flows. In Cebeci [41], 1982.

[52] J. Cousteix and R. Houdeville, "Singularities in three-dimensional turbulent boundary-layer calculations and separation phenomena," *AIAA*, vol. 19(8), pp. 976–985, 1981.

[53] E. Toro, *Riemann Solvers and Numerical Methods for Fluid Dynamics: A Pratical Introduction*. Springer, 3rd ed., 2009.

[54] N. Datta, *Numerical Linear Algebra and Applications*. SIAM-Society for Industrial and Applied Mathematics, 2nd ed., 2010.

[55] J. Strikwerda, *Finite Difference Schemes and Partial Differential Equations, Second Edition*. ASME, 2nd ed., 2004.

[56] J. Barbeau, *Polynomials*. Springer, 1989.

[57] M. Drela, "Xfoil: An analysis and design system for low reynolds number airfoils," in *Conference on Low Reynolds Number Airfoil Aerodynamics*, (University of Notre Dame), 1989.